1-1-2012

Functional Characterization Of The VAC14 Self-Interaction Domain

Tamadher A. Alghamdi
Ryerson University

FUNCTIONAL CHARACTERIZATION OF THE VAC14 SELF-INTERACTION DOMAIN

by

Tamadher Abdullah Alghamdi

Bachelor of Science

King Abdulaziz University, Jeddah, Saudi Arabia 2007

A thesis presented to Ryerson University

in partial fulfillment of the requirements for the degree of

Master of Science

in the program of Molecular Science

Toronto, Ontario, Canada, 2012

Author's Declaration

I hereby declare that I am the sole author of this thesis.

I authorize Ryerson University to lend this dissertation to other institutions or individuals for the purpose of scholarly research.

_____Tamadher_ ____

I further authorize Ryerson University to reproduce this dissertation by photocopying or by other means, in total or in part, at the request of other institutions or individuals for the purpose of scholarly research.

_____Tamadher_ ____

Abstract

FUNCTIONAL CHARACTERIZATION OF THE VAC14 SELF-INTERACTION DOMAIN

Tamadher Alghamdi, Master of Science in Molecular Science, Ryerson University, 2012

PtdIns(3,5)P_2 is a low-abundance signaling lipid present at < 0.1 % of total PtdIns lipids in yeasts and mammals. Reduced levels of PtdIns(3,5)P_2 contributes to neurodegenerative disorders in humans and vacuolar defects in yeasts. Steady-state levels of PtdIns(3,5)P_2 are dependent on both its rate of synthesis and turnover. In yeast, PtdIns(3,5)P_2 is produced on the vacuole membrane by phosphorylation of PtdIns(3)P at the 5 position of its inositol ring by the Fab1 lipid kinase. Cells lacking Fab1 make no PtdIns(3,5)P_2 and exhibit defects in vacuole morphology and function. The lipid phosphatase Fig4 counteracts Fab1 activity by turnover of PtdIns(3,5)P_2 into PtdIns(3)P. Vac14 is a regulatory protein implicated in the synthesis and turnover of PtdIns(3,5)P_2. It acts as an adaptor protein that controls both of Fab1 and Fig4 proteins. In addition, Vac14 exists as a multimer that allows for self-interaction. However, multimerization state of Vac14 as well as the domain responsible for self-interaction remained unknown. This study aimed to identify the self-interaction domain to elucidate its role in the assembly of the regulatory complex of PtdIns(3,5)P_2. The observations seen in this study suggested that Vac14 self-interacts via multiple conserved motifs in the C-terminus, which are crucial for interaction with Fab1 and Fig4, and the normal morphology of yeast vacuoles.

Acknowledgment

I would like to express my sincere gratitude to my supervisor, Dr. Roberto Botelho for his, guidance, rich knowledge and his continued support. His guidance and constructive feedback helped me develop a deeper understanding of the field, developing research skills and independence. He was always approachable and willing to help me through all stages of my research. His unique manner of combining discipline with his warm friendliness allowed me to be more productive in a comfortable collaborative environment. I would also like to thank my committee members, Dr. Jeffrey Fillingham and Dr. Marie Killeen for providing me with resources and insightful suggestions along the way.

In my daily work in the lab, I have been blessed with a friendly and cheerful group of fellow students, who made it a pleasant place to work. In particular, I would like to thank my friend and lab mate Shannon Ho for her collaboration and support to accomplish this project. I would also like to thank Amra Saric for establishing this project and for being there to share a laugh. Also special thanks to Danielle Taylor and Ahmad Sidiqi for giving me a hand when I needed it most and for being great friends. Everyone else who has helped me in one way or another from the Foster and Botelho labs, I thank you all dearly.

The generous support of the King Abdullah Foreign Scholarship Program that has made it possible for me to have this wonderfully rich academic experience is greatly appreciated. Outside of school, I have been fortunate to have a number of great friends who created a family-like environment for me. I thank them all for the doses of encouragement when they were needed.

Most of all, I am deeply grateful to have a wonderful, supportive and caring family for being my inspiration to succeed. I am especially indebted to my parents, my father Abdullah and my mother Norah, for their unconditional support and love throughout my studies. To them, I dedicate this thesis. Finally, my humble gratitude goes to God for giving me the strength to accomplish this.

Table of Contents

List of Tables

List of Figures

List of Abbreviations used

ALS	Amyotrophic lateral sclerosis
CMTD	Charcot-Marie-Tooth disease
CoIP	Co-immunoprecipitation
EEA1	Early endosome antigen 1
ESCRT	Endosomal sorting complexes required for protein transport
GST	Glutathione S-transferase
IP	Immunoprecipitation
MIP	Muscle-specific inositol phosphatase
MTMR14	Myotubularin-related protein 14
MVB	Multivesicular bodies
PH	Pleckstrin homology
PtdIns	Phosphatidylinositol
PtdIns(3)P	Phosphatidylinositol 3-phosphate
PtdIns(3,5)P_2	Phosphatidylinositol 3,5-bisphosphate
PtdIns(4)P	Phosphatidylinositol 4-phosphate
PtdIns(4,5)P_2	Phosphatidylinositol 4,5-bisphosphate
PX	Phox
RyR	Ryanodine receptor
TCA	Trichloroacetic acetic
TGN	Trans-Golgi network
TRPML1	Mucolipin transient receptor potential proteins

1 Introduction

1.1 Membrane trafficking

Eukaryotic cells have a variety of internal membrane structures called organelles that play roles in secretion and internalization of various molecules essential for functions such as cell growth, signal transduction, cytoskeletal dynamics and membrane trafficking.

Membrane trafficking refers to selective transport of cargos to various targets within or outside the cell by continuous exchange between membrane-bound vesicles (Bonifacino and Glick, 2004). The intracellular organelles communicate with each other through signal pathways to ensure that each molecule is selectively transported to the right target. This process follows highly organized directional route through four major steps: sorting, fission, targeting and fusion. Sorting involves selection of cargo, whereas fission involves budding from donor organelle. The delivery of the cargo is arbitrated by transport vesicles along microtubules or actin filaments, which facilitate the movement through cytoplasm (Rogers and Gelfand, 2000). The final step involves tethering in which the vesicle becomes into close proximity to the target membrane. Specific proteins such as small GTPases that are specifically localized on the organelle membrane mediate targeting the vesicles to the correct organelle by binding to effector proteins to form tethering complexes (Whyte and Murno, 2002). Tethering is followed by fusion with the donor oragnelle, which is mainly mediated by conserved core protein machinery known as SNARE (soluble N-ethylmaleimide-sensitive factor attachment protein receptors) (Gonzalez and Scheller, 1999).

Endocytic and secretory pathways are two major pathways in membrane trafficking that play a major role in maintaining the homeostasis of the cell. The secretory pathway involves synthesis

of proteins and lipids in the endoplasmic reticulum (ER), which are then transported in vesicles to the Golgi apparatus for further processing and sorting to various destinations. In comparison, the endocytic pathway, also known as endocytosis, internalizes molecules from the plasma membrane and targets them to endosomes and lysosomes for degradation (Bonifacino and Glick, 2004). Figure 1.1 shows summary of the main membrane trafficking pathways.

1.2 The endocytic pathway

The endocyitc pathway begins with recognizing extracellular ligands such as low-density lipoprotein (LDL) and transferrin, which bind to their corresponding receptors on the plasma membrane for further internalization of irons and cholesterol, respectively (Figure 1.1) (Dohetry and McMahon, 2009). The formed ligand-receptor complex will initiate recruitment of coat proteins such as clathrin and adaptor protein 2 (AP2) from the cytosolic region (Schekman and Orci, 1996). The recruitment of clathrin causes a small portion of the plasma membrane to bud and form an endocytic vesicle that is targeted to early endosomes. After uncoating of clathrin coat proteins, the naked endocytic vesicle fuses with the early endosomes, which have tubular shape and acidic pH for sorting internalized molecules either to late endosomes and lysosomes for digestion, or back to the plasma membrane for recycling. The acidity of the early endosomes ($pH \approx 6$) causes dissociation of receptors from their ligands (Mellman, 1992). Recycled molecules such as transferrin-receptor that released Fe^{3+}, are transported to the plasma membrane via recycling endosomes (Maxfield and McGraw, 2004). Composition of some transmembrane receptors like EGF-receptor and signaling proteins such as ubiquitin specifically target cargoes for degradation (Piper and Luzio, 2001). The sorting machinery in the early endosomes recognizes ubiquitin-tagged molecules such as epidermal growth factor receptors

(EGFRs)(Maxfield and McGraw, 2004; Katzmann et al., 2002). As the early endosomes mature to late endosomes, ESCRT (endosomal sorting complex required for transport) machinery recognizes ubiquitin-tagged cargoes destined for degradation, which are then sorted into internal vesicles, known as multivesicular bodies (MVBs) (Katzmann et al., 2002). Cargoes enter MVB pathway are then delivered to lysosomes for degradation by hydrolytic enzymes (Piper and Luzio et al., 2001).

The dynamic nature of these organelles raises major questions: What are the molecular mechanisms that mediate the accurate direction of transport vesicles to the correct organelles? And how do cells maintain organelle identity while exchanging membranes and contents?

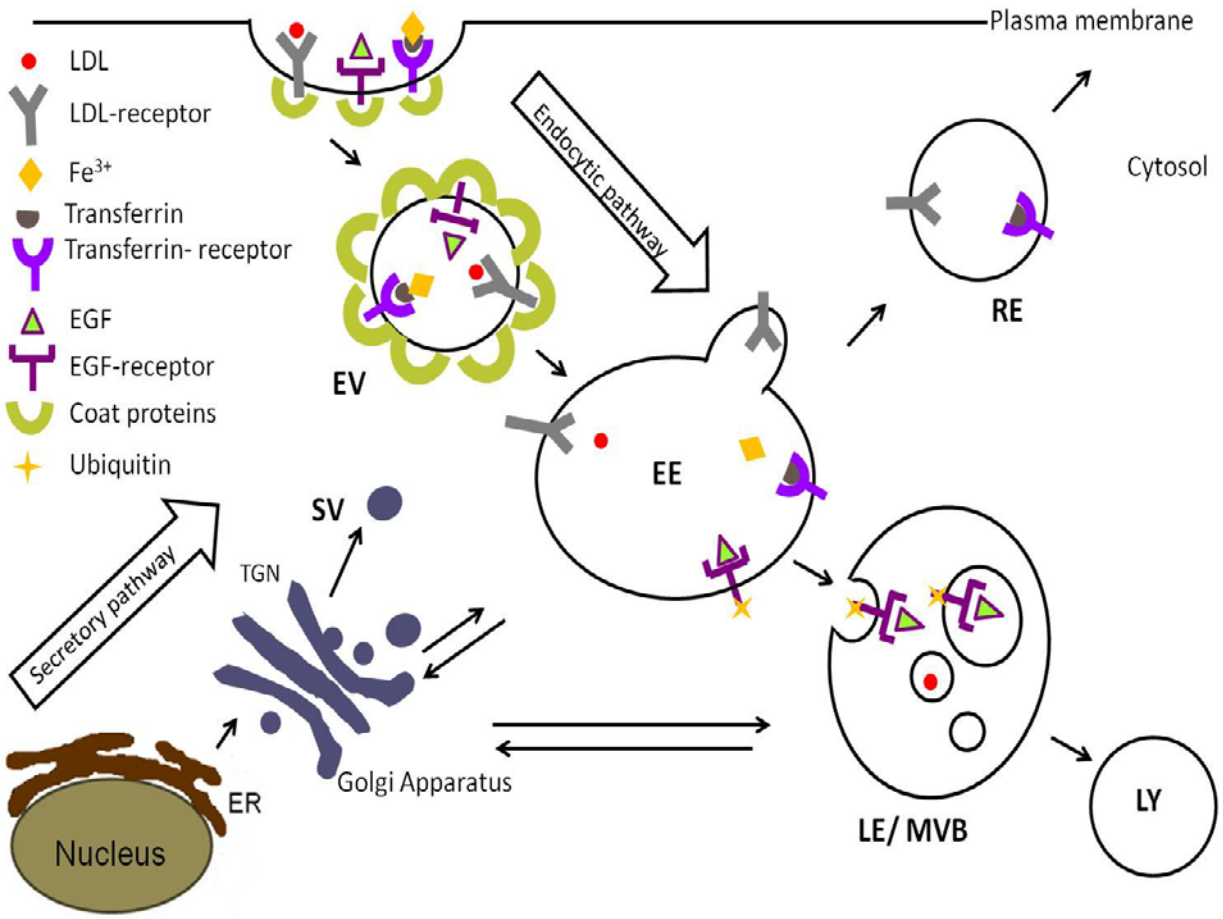

Figure 1.1. Membrane trafficking in eukaryotic cell. The schematic diagram shows the major pathways in membrane trafficking including secertory and endocytic pathways. The seceretory pathway begins in Endoplasmic reticulum (ER), where proteins and lipids are synthesized and sent to Golgi to be packed and secreted from *trans*-Golgi network (TGN) via secretory vesicles (SV) to the plasma membrane. Endocytic pathway starts with recognition of ligands by specific receptors on the plasma membrane to form a complex. Examples of internalized cargos are shown. Cargos destined for endocytosis triggers invagination of a small portion of the plasma membrane and recruitment of coat proteins to form an endocytic vesicle (EV). Coat proteins are removed and the naked EV fuses with early endosome (EE) for sorting of internalized molecules. Some molecules such as LDL- and transferrin-receptors are recycled back to the plasma membrane via recycling endosome (RE). As the early endosome matures to late endosome, mono-ubiquitinated molecules such as EGF-receptor and the remaining molecules destined for degradation are internalized into small internal vesicles known as multiviscular bodies (MVB). Molecules are then sent for degradation in the lysosome (LY) by specific hydrolytic enzymes. The possible fates involved in membrane trafficking are shown in solid arrows.

1.3 Organelle identity

In eukaryotic cells, each organelle has distinctive shape, composition and function. The accuracy of membrane trafficking depends on the correct targeting and recognition of the internal organelles (Behnia and Munro, 2005). Many of the proteins that decorate the organelle membranes are not integral, they are peripheral proteins instead. The peripheral proteins including the various coat proteins, motor proteins and tethering factors, are directly recruited to the cytosolic surface of the organelles. Each organelle membrane has a specific set of effector proteins that preserve its identity for accurate functioning (Behnia and Munro, 2005). A key question is how are these peripheral-membrane proteins recruited and regulated to generate organelle identity and function?

There are two main key determinants for organelle identity: small GTPases of the Arf and Rab family of proteins and the lipid phosphoinositides, which are phosphorylated forms of phosphatidylinositol (PtdIns). The specific distribution and localization of PtdInsPs and small GTPases within the organelle membranes provide identity code for each organelle. Cooperation of PtdInsPs with small GTPases regulates membrane trafficking by recruitment of highly specific cytosolic proteins, which provide a unique function and identity for each organelle (Behnia and Munro, 2005).

1.3.1 Phosphoinositides (PtdInsPs)

PtdInsPs are phospholipids produced by phosphorylation of PtdIns, on the 3, 4 or 5 positions of the inositol ring. PtdIns is a phospholipid consists of inositol polar head group that is attached to two non-polar fatty acid tails via phosphate group with a glycerol backbone (Figure 1.2A). Phosphorylation of the inoistol head group generates seven PtdInsPs species (Figure

1.2B)(Vicinanza et al., 2008; Di Paolo and De Camilli, 2006). A range of lipid kinases and phosphatases mediate the phosphorylation and dephosphorylation of the head group, respectively. The concerted action of the kinases and the phosphatases, determine the spatial restriction and steady-state levels of each PtdInsP (Di Paolo and De Camilli, 2006). PtdInsPs are specifically distributed in different organelles, with phosphatidylinositol 4-phosphate (PtdIns(4)P) predominate on Golgi, phosphatidylinositol 4,5-bisphosphate (PtdIns(4,5)P_2) generated at the plasma membrane, phosphatidylinositol 3-phosphate (PtdIns(3)P) on early endosomes, and phosphatidylinositol 3,5-bisphosphate (PtdIns(3,5)P) found on late endocytic organelles (Di Paolo and De Camilli, 2006). Each PtdInsP binds to specific effector proteins. The interactions between cytosolic proteins and PtdInsPs are typically mediated by specialized conserved protein domains such as FYVE, Phox homology (PX) and pleckstrin homology (PH) (Hurley and Misra, 2000). For example, PtdIns(4,5)P_2 is produced locally at the plasma membrane where it binds to coat proteins such as AP2 and dynamin via its PH domain to initiate endocytosis and actin cytoskeleton arrangement (Honing et al., 2005; Martin, 2001). Moreover, cooperation of PtdInsP s with small GTPases increase the affinity of organelle membranes for peripheral proteins essential for various events in membrane trafficking. For example, PtdIns(3)P on early endosomes binds to Early Endosome Antigen 1 (EEA1), Rab5-GTP effector protein, through its conserved binding domain, FYVE zinc finger to mediate endosomes fusion (Simonsen et al., 1998). PtdInsPs play essential roles in membrane trafficking; therefore, their regulations and functions are continued to be studied.

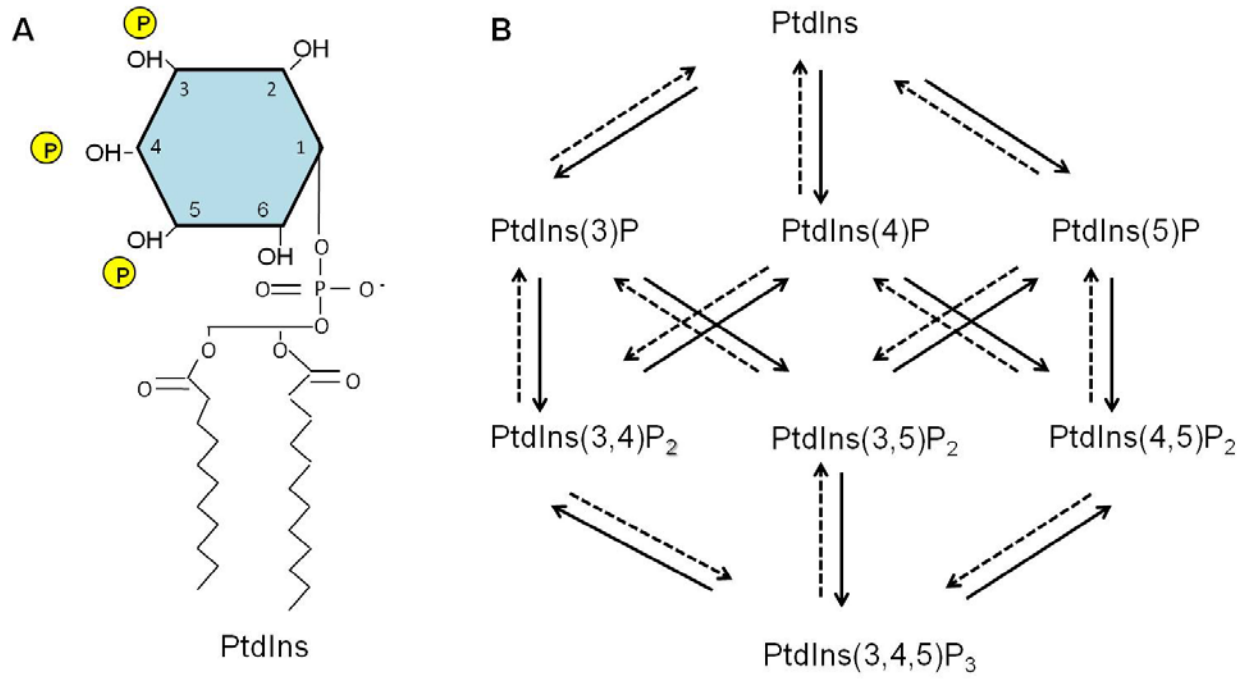

Figure 1.2. Phosphatidylinositol structure and its derivatives, phosphoinositides. A. Phosphatidylinositol (PtdIns) consists of inositol polar head group that is linked to two non-polar fatty acid tails via phosphate group with a glycerol backbone. Phosphorylation of the inositol ring on the 3, 4 or 5 positions individually or in combination, generates seven PtdInsPs. The possible positions of phosphate group are shown in yellow. **B.** Phosphoinositides (PtdInsPs), the derivatives of (PtdIns) are shown. Straight and dotted arrows indicate the phosphorylation and dephosphorylation pathways of each PtdInsP, respectively. Modified from (Di Paolo and De Camilli, 2006).

1.4 Phosphatidylinositol-3,5-bisphosphate (PtdIns(3,5)P_2)

PtdIns(3,5)P_2 is a low-abundance signaling lipid, contributing < 0.1% of the total PtdIns lipids, found in yeast vacuoles and in endolysosomes of higher eukaryotes (Dove et al., 1997). During endolysosome trafficking, PtdIns(3)P is phosphorylated to PtdIns(3,5)P2 by the kinase Fab1, also known as PIKfyve, on the vacuolar/endosomal membrane in yeasts and mammals, respectively. Despite the low abundance of PtdIns(3,5)P2 at the vacuolar/endosomal membrane, its steady-state level is essential to maintain and regulate the vacuolar/endosomal morphology and function (Dove et al, 1997; Efe, 2007; Whiteford et al., 1997).

In yeast, PtdIns(3,5)P_2 plays several roles in maintaining cellular functions such as vacuole acidification, membrane recycling and MVBs protein sorting. Low levels of PtdIns(3,5)P_2 results in swollen vacuoles and defective retrograde trafficking from the vacuole (Figure 1.3A)(Odorizzi et al., 1998; Yamamoto et al., 1995, Gary et al., 1998). Conversely, elevated levels of PtdIns(3,5)P_2 in response to hyperosomotic stress display shrinkage and fragmentation in yeast vacuoles thereby inducing exit of vacuolar solutes and water, suggesting that PtdIns(3,5)P_2 plays a significant role in response to osmotic stress (Gary et al., 1998; Duex et al., 2006; Gary et al., 2002; Bonangelino, 2002).

In mammals, PtdIns(3,5)P_2 controls events associated with endosomal compartments (Ikonomov et al., 2002). PtdIns(3,5)P_2 deficient-cells exhibit similar phenotypes shown in yeast such as enlarged endosomes and defective endosomes-to-TGN retrograde trafficking (Sbrissa et al., 2000; Nicot et al., 2006; Rusten et al., 2006; Jin et al, 2008). Mutations in PtdIns(3,5)P_2 regulatory proteins that lead to reduced level of PtdIns(3,5)P_2, contribute to neurodegenerative disorders such as Charcot-Marie-Tooth disease (CMTD) and amyotrophic lateral sclerosis (ALS) (Figure 1.3B and C) (Chow et al., 2009; Chow et al., 2007; Zhang et al., 2008).

PtdIns(3,5)P_2 was recently found to be involved in regulating the mucolipin transient receptor potential proteins (TRPML), which are channels for Ca^{+2} release in endolysosomes (Lange et al., 2009; Dong et al., 2010). TRPML1 deficient cells display similar phenotype as cells with low level of PtdIns(3,5)P_2, including enlarged endolysosomes and defective trafficking in the late endocytic pathway (Cheng et al., 2010; Puertollano and Kiselyov, 2009). According to Dong et al., PtdIns(3,5)P_2 activates TRPML1 by binding to its N-terminus to regulate Ca^{+2} release, which stimulates membrane fission and fusion events (2010). Interestingly, overexpression of TRPML1 in mouse fibroblasts that lack PtdIns(3,5)P_2 was found to rescue the

swollen endolysosome phenotype, while increased level of PtdIns(3,5)P_2 accelerated Ca^{+2} release into the cytosol (Dong et al., 2010). Regulated level of PtdIns(3,5)P2 was also shown to be significantly involved in maintaining Ca^{+2} homeostasis in skeletal and heart muscle cells by direct binding to the Ca^{2+} release channel, ryanodine receptor 1(RyR1) in sarcoplasmic reticulum (Shen et al, 2009). The recently identified muscle-specific inositol phosphatase/ myotubularin-related protein 14 (MIP/MTMR14) expressed in skeletal and heart muscles, mediates dephosphorylation of PtdIns(3,5)P_2 and has a crucial role in maintaining Ca^{2+} homeostasis in skeletal muscle (Wishart et al., 2002; Shen et al, 2009). Mice deficient in MIP exhibited abnormal muscle function that caused weakness and fatigue in skeletal muscles. This was elucidated by the accumulation of PtdIns(3,5)P_2 in MIP deficient cells, which leads to leakage of Ca^{2+} from the sarcoplasmic reticulum (Shen et al, 2009). Based on these findings, Touchberry and colleagues hypothesized that PtdIns(3,5)P2 could also be involved in cardiac muscle contractility (2010). Their data showed that elevation of PtdIns(3,5)P_2 increases contraction in cardiac muscle by direct activation of the RyR2 channel (Touchberry et al., 2010). These observations suggest a potential role of PtdIns(3,5)P_2 in regulation of ion channels and that Ca^{+2} is an effector of PtdIns(3,5)P_2.

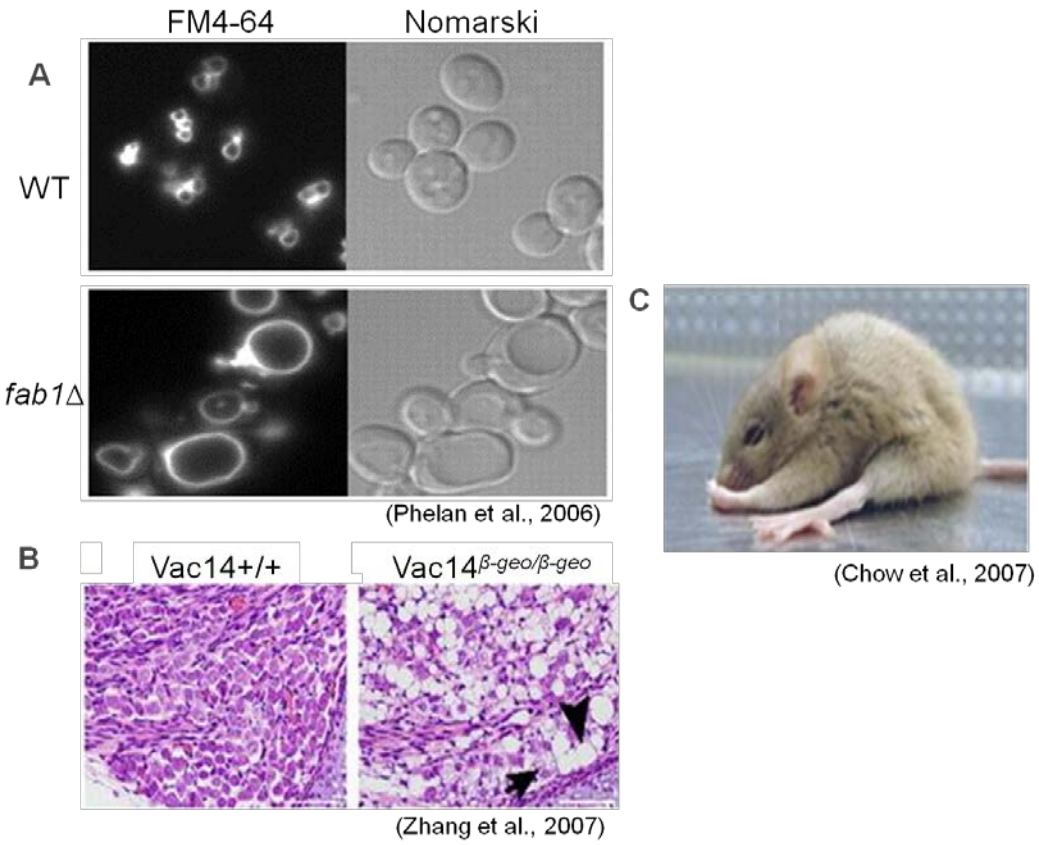

Figure 1.3. Deficiency of PtdIns(3,5)P_2 levels in yeasts and mammals. A. Vacuolar morphology of wild type yeast cells (WT) and *fab1*Δ cells which has no PtdIns(3,5P_2. Yeast cells that lack PtdIns(3,5)P_2 have enlarged, single-lobed vacuoles compared to WT (Phelan et al., 2006). **B.** Morphology of neural tissue from Vac14$^{\beta\text{-}geo\text{-}\beta\text{-}geo}$, a mutant mice that lack Vac14, the positive regulator of PtdIns(3,5)P_2. The cell bodies have large intracellular vacuoles (arrowheads) (Zhang et al., 2007). **C.** The *pale tremor* mouse (*plt*), shows peripheral neuropathy caused by mutation in Fig4, the lipid phosphatase (Chow et al., 2007).

1.5 Regulation of PtdIns(3,5)P_2

Steady-state level of PtdIns(3,5)P_2 is dependent on both its rate of synthesis and turnover. A variety of regulatory proteins involved in regulation of PtdIns(3,5)P_2 have been identified to better understand the functions of PtdIns(3,5)P_2. In yeast, PtdIns(3,5)P_2 is produced on the vacuole membrane by phosphorylation of PtdIns(3)P at the 5-hydroxyl group of its inositol ring by the lipid kinase, Fab1 (Figure 1.4)(Gary et al, 1998). Yeast cells lacking Fab1 make no PtdIns(3,5)P_2 and exhibit defects in vacuole morphology and acidification (Figure 1.3A)(Cooke

et al, 1998;Gary et al, 1998). Another positive regulator protein involved in PtdIns(3,5)P_2 regulation is Vac7, which is found only in yeasts and mediates regulation of Fab1 activity by an unknown mechanism (Gary et al., 2002). PtdIns(3,5)P_2 level is undetectable in *vac7*Δ cells suggesting that Vac7 plays an essential role in PtdIns(3,5)P_2 synthesis (Gary et al., 2002).

The lipid phosphatase, Fig4, is localized on the vacuolar membrane acting as a negative regulator of PtdIns(3,5)P2 (Rudge et al, 2004). Fig4 counteracts Fab1 activity by dephosphorylation of PtdIns (3,5)P_2 into PtdIns(3)P (Figure 1.4)(Gary et al, 2002). The level of PtdIns (3,5)P_2 is also controlled by recruitment of Atg18, an effector protein that acts a negative regulator of the Fab1 kinase pathway. *atg*Δ yeast cells typically exhibit 10-fold increase in PtdIns(3,5)P_2 levels (Bryant and Stevens, 1998 ; Dove et al., 2004). Vac14 is another regulatory protein implicated in both synthesis and turnover of PI(3,5)P_2 by acting as an adaptor protein that controls both Fab1 and Fig4 proteins (Figure 1.4)(Duex et al., 2006). Homologues of Fab1p, Fig4p and Vac14p are conserved in higher eukaryotes and are known as PIKfyve, Sac3 and ArPIKfyve, respectively (Ikonomov et al, 2009; Rutherford et al, 2006). Moreover, the mammalian orthologs of Atg18 are WIPI proteins involved in autophogy (Proikas-Cezanne et al., 2004; Polson et al., 2010).

To further understand the molecular mechanism implicated in PtdIns(3,5)P_2 regulation, I highlight the structure and function of the main regulatory components of PtdIns(3,5)P_2 .

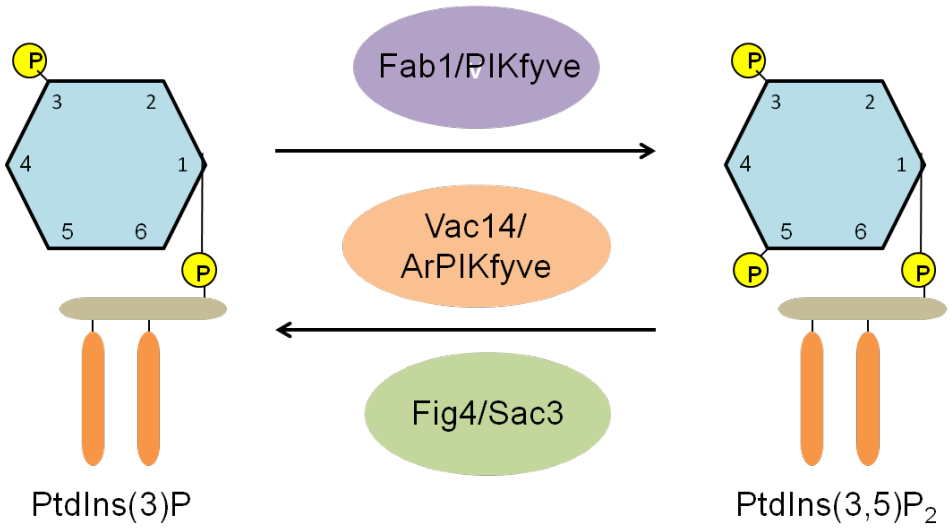

Figure 1.4 PtdIns(3,5)P_2 synthesis and turnover. PtdIns(3,5)P_2 is synthesized by the lipid kinase Fab1/PIKfyve, which phosphorylates PtdIns(3)P on the 5-hydroxyl group of its inositol ring. The lipid phosphatase Fig4/Sac3 mediates dephosphorylation of PtdIns(3,5)P_2 into PtdIns(3)P. Synthesis and turnover is regulated by the adaptor like protein Vac14/ArPIKfyve.

1.5.1 Fab1: the lipid kinase

FAB1, the gene encoding the 257-kD protein kinase Fab1, is required for the synthesis of PtdIns(3,5)P_2 (Efe et al., 2005; Michell et al., 2006). The Fab1 protein is located on the vacuolar membrane in yeast, whereas its mammalian orthologue, PIKfyve, is found on endosomes/lysosomes (Gary et al., 1998; Ikonomov et al., 2001). Fab1 consists of several conserved domains including a cysteine-rich FYVE domain in the N-terminus, the CCT and CCR domains, and a kinase domain at the C-terminus (Figure 1.5A)(Efe et al., 2005; Michell et al., 2006). The FYVE domain of Fab1 is required for binding to its substrate, PtdIns(3)P on the vacuolar/endolysosomal membrane (Burd et al., 1998; Botelho et al., 2008; Sbrissa et al.,2002). The CCT and CCR domains are part of GroL superfamily involved in folding of actin and tubulin, and are important for Fab1 function (Michell et al., 2006; Botelho et al., 2008). In yeast, disrupting the CCT and CCR domains (Grol-related region) of Fab1 caused a decrease in PtdIns(3,5)P_2 by ~60-80% and defective vacuolar morphology and function (Figure

1.5B)(Botelho et al., 2008). Consistent with these findings, Sbrissa et al. also showed that deletion of CCT domain in mammalian cells impaired the PIKfyve activity (2008). In addition, the GroL-like domain of Fab1 acts as a binding site for Vac14 and Fig4 in yeast and mammals (Botelho et al., 2008, Ikonomov et al., 2009).

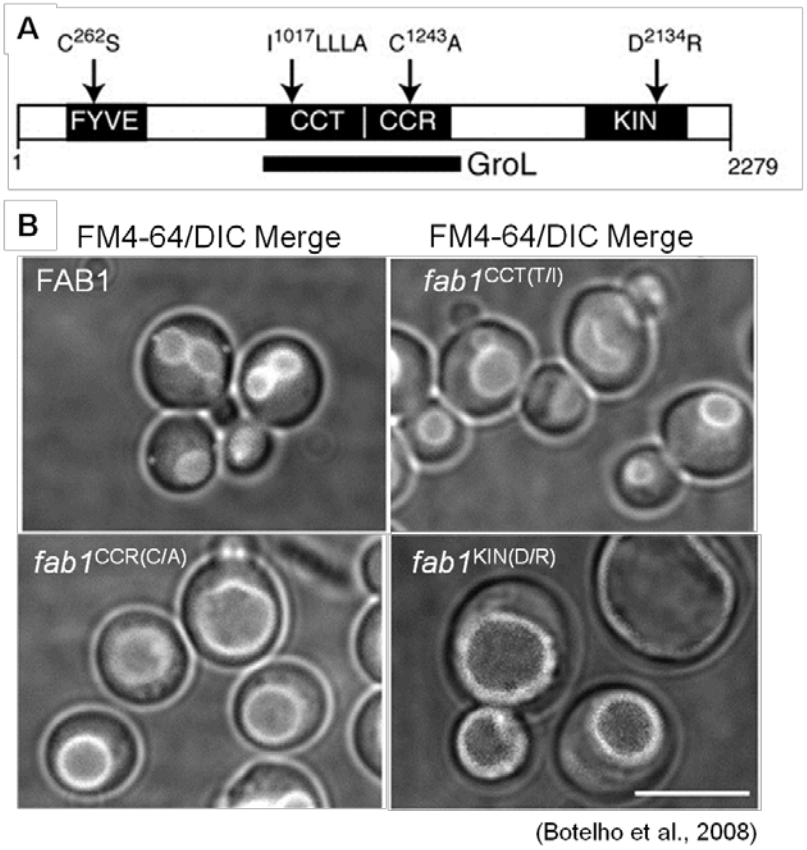

Figure 1.5. Effect of disruptive domains of Fab1 on the vacuolar morphology. A. Diagram represents the Fab1 domains including FYVE, CCT,CCR (GroL) and KIN. Point mutations created into each domain are indicated above. **B.** Vacuolar morphology of yeast cells of *fab1*Δ expressing wild type (FAB1) or Fab1 mutants including *fab1* $^{CCT(T/I)}$,*fab1* $^{CCR(C/A)}$, *fab1* $^{(KIN\ (D/R)}$ display enlarged vacuoles compared to wild type.

1.5.2 Fig4: the lipid phosphatase

Fig4 consists of a phophatase domain known as Sac1 domain, which is conserved in several proteins that have phosphoinositide phosphatase activities (Guo et al., 1999; Rudge et al., 2004; Zhong and Zheng-Hua, 2003). The phosphatase activity of Fig4 is required for turnover of

PtdIns(3,5)P_2 at 5-hdroxyl group (Duex et al., 2006; Rudge et al., 2004). In yeast, association of Fig4 on the vacuolar membrane is also required for PtdIns(3,5)P_2 synthesis. Surprisingly, deletion of *FIG4* in yeast cells displayed reduced level of PtdIns(3,5)P_2 upon stimulation by hyperosmotic shock, which normally causes 20-fold elevation of PtdIns(3,5)P_2 levels (Duex et al., 2006).

However, inhibition of phosphatase activity of Fig4 displayed increase level of PtdIns(3,5)P_2 compared to wild-type and *fig*Δ cells. Similar observations were seen in *atg18*Δ *fig4*Δyeast cells in which deletion of *FIG4* prevented the elevated levels of PtdIns(3,5)P_2 in *atg18*Δ, while expression of *fig4-1* phosphatase-dead allele resulted in PtdIns(3,5)P_2 levels higher than deletion of *ATG18* alone (Botelho et al., 2008). In contrast, the expected increase levels of PtdIns(3,5)P_2 was observed upon deletion of Fig4 in mammalian cells (Sbrissa et al., 2007). These observations suggested that Fig4 plays a dual function in PtdIns(3,5)P_2 regulation. The phosphatase activity of Fig4 promotes turnover of PtdIns(3,5)P_2 while the Fig4 protein itself is essential for PtdIns(3,5)P_2 synthesis (Gary et al., 2002; Botelh et al., 2008). Interestingly, pale tremor mice, a model of CMTD type 4J (CMT4J), illustrated the first linkage of the reduced amounts of PtdIns(3,5)P_2 caused by mutations of *FIG4* to neurodegenerative disorders (Figure 1.3C) (Chow et al., 2007). Vacuolation of the neurons along with endosomal enlargement were observed in both the mouse model and patients with CMT4J (Figure 1.3C)(Chow et al., 2007; Zhang et al., 2008)

1.5.3 Vac14: an adaptor like protein

Vac14 consists of 880 residues with a mass of ~ 100 kDa and is integral to control the basal levels of PtdIns(3,5)P_2 (Bonangelino et al., 1997; Dove et al., 2002). Its orthologs are

widely distributed from yeasts to mammals (Bonangelino et al.,2002; Dove et al., 2002). Vac14 was first identified by monitoring the levels of PtdIns(3,5)P_2 in response to osmotic stress in yeast (Bonangelino, 2002). During exposure to hyperosmotic stress, Vac14 appears to act as an osmosensor and activates Fab1, which stimulates the 20-fold increase of PtdIns(3,5)P_2 levels (Bonangelino, 2002). Moreover, deletion of *VAC14* reduced the levels of PtdIns(3,5)P_2 by approximately 10% resulting in an abnormal vacuolar morphology such as single-lobed and enlarged vacuoles, the typical phenotype observed in *fab1*Δ yeast cells (Dove et al., 2002; Bonangelino et al., 2002). Likewise, mammalian cells that lack Vac14 display decreased levels of PtdIns(3,5)P_2 and enlarged endolysosomes (Zhang et al., 2007; Jin et al., 2008). These observations resemble the morphological abnormality observed in endosomes upon expression of PIKfyve kinase-defective dominant-negative (Ikonomov et al., 2003). In addtion, loss of Vac14 in mice causes neurodegeneration in central and peripheral nervous systems (Zhang et al., 2007). The mouse model that lacks Vac14 protein, *Vac14*$^{\beta\text{-geo}/\beta\text{-geo}}$ has decreased PtdIns(3,5)P_2, vacuolation in the affected neurons and defective retrograde trafficking pathway from endosomes (Figure 1.3B) (Zhang et al., 2007). These observations stress the importance of understanding the molecular function of Vac14 and how it regulates PtdIns(3,5)P_2.

Vac14 acts as a scaffold for the PtdIns(3,5)P_2 regulatory complex, also known as the Fab1 complex (Botelho et al., 2008). Sequence analysis of Vac14 using REP, a bioinformatic program that searches a protein sequence for repeats, revealed that Vac14 is composed of at least 9 and up to 21 HEAT repeats, which are helix-loop-helix motifs (Figure 1.6 A and B)(Dove et al, 2002; Jin et al, 2008). HEAT repeats are found in several proteins including the four name-giving proteins, Huntingtin, elongation factor 3 (EF3), protein phosphatase 2A (PP2A), and the yeast PI3-kinase TOR1, and are involved in mediating protein-protein interaction (Figure 1.6C) (Andrade et al.,

2001; Vetter et al., 1999). The existence of HEAT repeats in Vac14, suggests that it interacts with PtdIns(3,5)P_2 regulatory proteins such as Fab1 and Fig4.

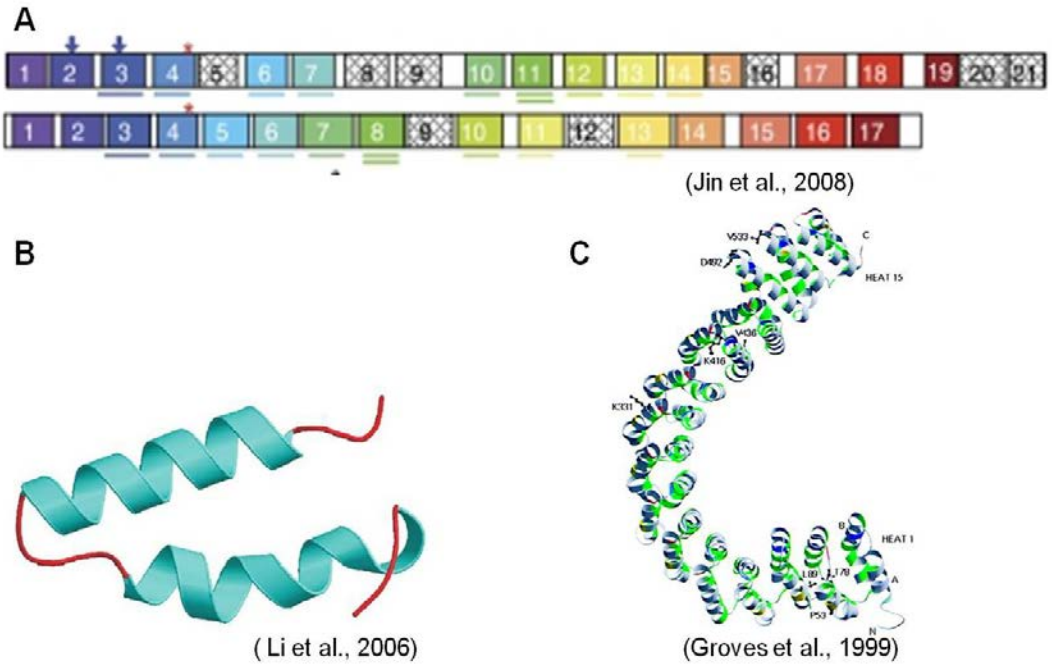

Figure 1.6. Model of HEAT repeats and the expected number of HEAT motifs in yeasts and mammals . **A**. Number of HEAT repeats in Vac14 in yeast (top) and mammals (bottom). **B.** A single HEAT repeat unit consists of two parallel helices connected by an intra-loop unit (helix-loop-helix), allows for conformational changes. **C.** Structure of HEAT repeats-containing protein, phosphatase 2A, which consists of PR65/A subunit containing 15 tandems HEAT repeats.

1.6 The Fab1 complex

In yeast, the Fab1 kinase forms a complex with Vac14 and Fig4 on the vacuole membrane (Figure 1.7A) (Rudge et al., 2004; Botelho et al., 2008). This was revealed by previous co-immunoprecipitation (coIP) analysis which showed that Fab1 binds indirectly to Fig4 through Vac14 on the Fab1 complex, while Vac14 and Fig4 bind to each other independently of Fab1 (Botelho et al., 2008). However, in *vac14*Δ cells, the Fab1 kinase and Fig4 phosphatase do not bind, which reveals that Vac14 acts as a linker between Fab1 kinase and Fig4 phosphatase (Botelho, 2008). Moreover, in *fab1*Δ cells, Vac14 and Fig4 remained bound suggesting that they

bind independently of Fab1. These findings were compatible with the mammalian orthologs of the Fab1complex components, PIKfyve, ArPIKfyve andSac3 (PAS complex) (Figure 1.7B)(Sbrissa et al., 2007; Sbrissa et al., 2008). However, the molecular mechanism that permits the Fab1 kinase and its regulatory proteins including Vac14 and Fig4 to form the Fab1 complex is yet to be understood (Botelho et al, 2008).

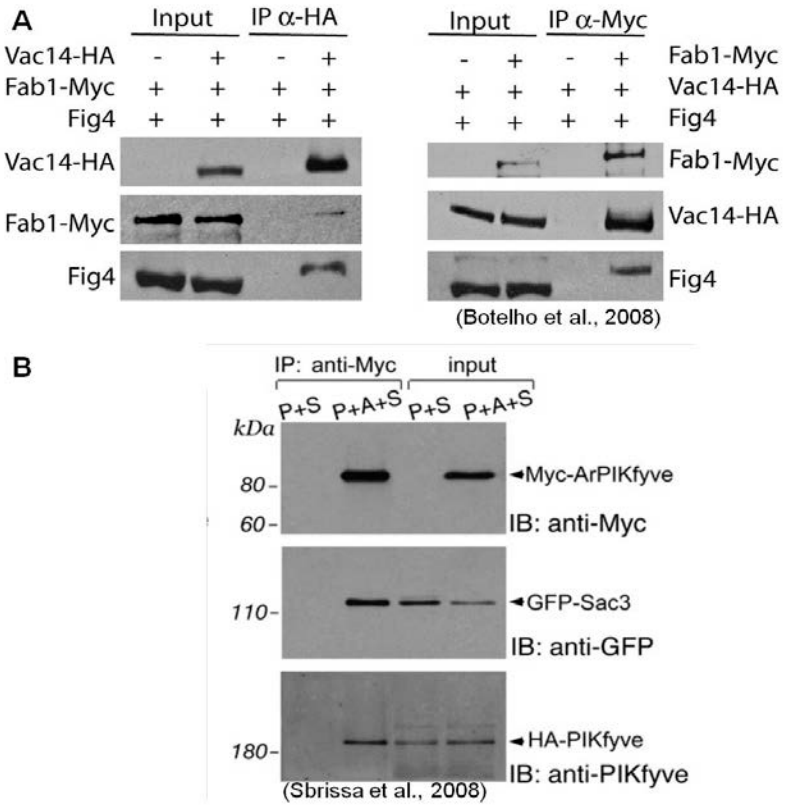

Figure 1.7. Interaction of the regulatory components of Fab1 complex in yeast and mammalian cells A. Fab1, Fig4 and Fab1 interact to form Fab1 complex in yeast cells. CoIP of whole cell lysates from yeast cells expressing Vac14-HA, Fab1-myc and Fig4. Monoclonal anti-HA (left) or anti-Myc (right) were used for IP from whole cell lysates, followed by SDS-PAGE and western blot. Input lanes represent 10% of the total material used for each IP (Botelho et al., 2008). **B.** PIKfyve, ArPIKfyve and Sac3 interact to form PAS complex, the mammalian homolog of Fab1 complex. CoIP of mammalian cells cotransfected with HA-PIKfyve + Myc-ArPIKfyve + eGFP-Sac3. Anti-myc antibodies were used for IP, followed by SDS-PAGE and western blot. Blots were immunoblotted as indicated. P, PIKfyve; A, ArPIKfyve; S, Sac3; IB, immunoblotting (Sbrissa et al., 2008).

1.7 Vac14 multimerization

Although it was known that Vac14 is required for PtdIns(3,5)P2 synthesis and degradation, the exact molecular mechanism of dividing Vac14 function remains to be understood. Unlike Fab1 and Fig4, Vac14 exist as a multimer in yeast and mammals (Dove et al., 2002; Jin et al., 2008; Botelho, 2008; Sbrissa et al., 2008).

In yeast, coIP from whole cell lysates expressing two copies of Vac14 tagged with different epitopes showed that Vac14 self-interacts (Figure 1.8A) (Botelho et al., 2008). These findings were consistent with two-hybrid analysis, which also showed that Vac14 interacts with itself (Dove et al., 2002; Jin et al., 2008). Moreover, direct self-interaction of Vac14 was confirmed in vitro using bacterially expressed recombinant GST-Vac14. T7-Vac14-HIS was recovered with GST-Vac14 coupled to glutathione-agarose beads (Figure 1.8B). The exact multimerization state of Vac14 remains elusive. However, a recent Master's thesis research by my colleague, Shannon Cheuk Ying Ho, suggested that Vac14 is a homodimeric and/ or homotrimeric protein.

Multimerization of Vac14 has also been shown in the mammalian homolog, ArPIKfyve (~ 82 kDa) (Sbrissa et al., 2008). Sibrissa et al used several approaches to test ArPIKfyve homomeric interaction. The coIP analysis of cells transfected with ArPIKfyve constructs tagged with different epitopes including eGFP-HA and Myc, displayed positive interaction between eGFP-HA-ArPIKfyve and Myc-ArPIKfyve (Sibrissa et al., 2008). Moreover, in vivo cross-linking in cells expressing wild-type ArPIKfyve showed ~170- and ~250-kDa cross-linked bands, suggesting that ArPIKfyve might form a dimer or trimer (Figure 1.8C). The multimerization was shown to be mediated by the C-terminal half of ArPIKfyve. Interestingly, disruption of ArPIKfyve self-interaction result in dissembly of the PAS complex and PIKfyve

activity, suggesting that Vac14 multimerization is essential (Sibrissa et al., 2008).

Although Vac14 multimerization occurs in yeast and mammals, the exact self-interaction motifs as well as the functional relevance remain undetermined. Therefore, much remains to be worked out including, how many copies of Vac14 exist on the Fab1 complex, what is the domain that is responsible for Vac14 self-interaction and whether this interaction is important for the function and assembly of the Fab1 complex on the vacuole membrane.

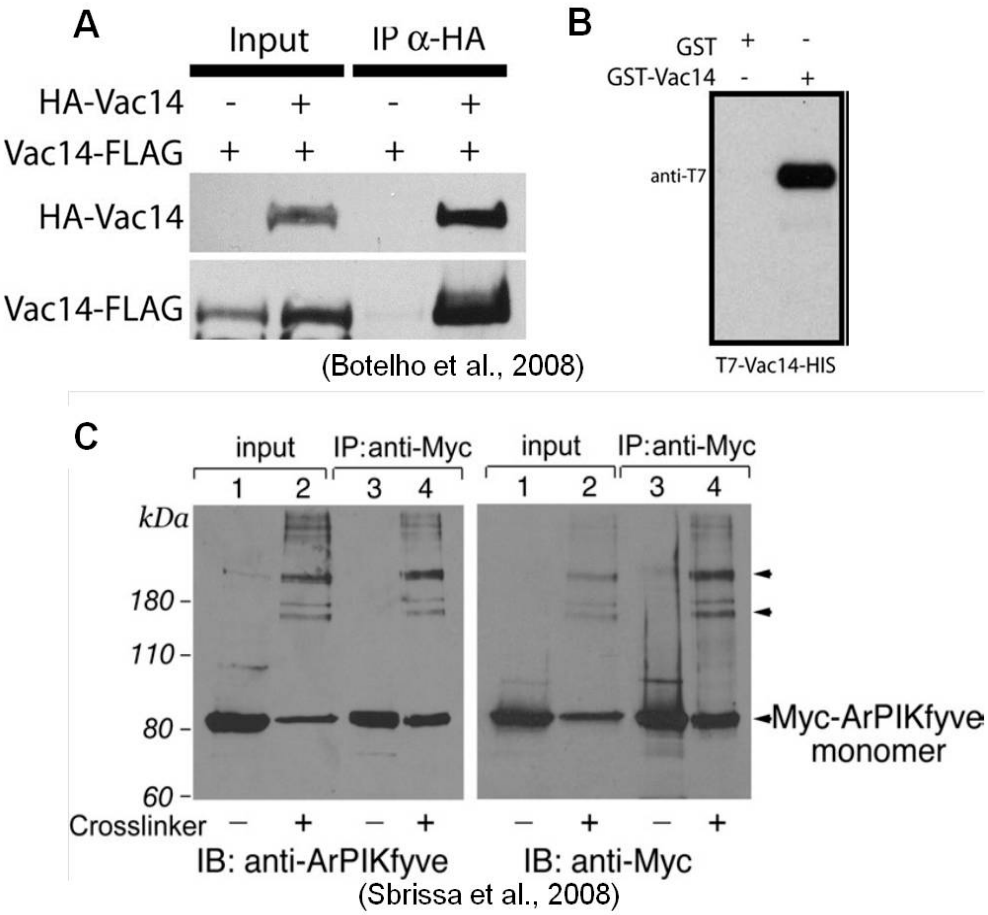

Figure 1.8 Vac14 multimerization. A. IP with anti-HA antibodies from whole cell lysates from yeast cells expressing Vac14-FLAG and HA-Vac14, followed by SDS-PAGE and western blot. Input lanes represent 10% of the total material used for IP. **B.** In vitro Vac14 self-interaction. GST and GST-Vac14 coupled to glutathione agarose beads were incubated with T7-Vac14-HIS_6. Blots were probed with monoclonal anti-T7 antibodies. **C.** In vivo cross-linking was performed with free-methanol formaldehyde for mammalian cells transfected with Myc-ArPIKfyve. Lysates were immunoprecipitated with anti-Myc antibodies, followed by SDS-PAGE and western blot. Cross-linked bands corresponding to 170 and 250 kDa, display homodimeric or homotrimeric interactions, respectively (arrowheads).

1.8 Hypothesis

Multimerization of Vac14 protein complex is essential for the assembly of Fab1 complex and subsequently for regulation of PtdIns(3,5)P_2. For this study, the main goal is to identify and functionally characterize the self-interaction domain of Vac14 using the following objectives:

1.9 Objectives

1. Test expression of FLAG-tagged Vac14 truncated mutants
2. CoIP of HA-tagged full length wild-type Vac14 with FLAG-tagged Vac14 truncations to “estimate” the self-interaction region
3. Create point mutations within the putative region of Vac14-self interaction and retest for expression and CoIP again full length of Vac14 to identify the self-interaction motifs
4. Demonstrate if Vac14 multimerization is essential for the function of Fab1 and Fig4, and consequently for the regulation of PtdIns(3,5)P_2

2 Materials & methods

2.1 Bacterial strains

All bacterial strains in this study were acquired by transformation into DH5α competent cells, and were used for DNA isolation and cloning purposes.

2.2 Yeast strains

The *Saccharomyces cerevisiae* strains used in this study and their genotypes are listed in Table 1.

Table 2.1 *S. cerevisiae* strains employed in this study

Strain name	Genotype	Reference or source
wild type (SEY6210)	Matα *leu*2-3, 112 *ura*3-52 *his*3-Δ200 *trp*1-Δ901 *lys*2-801 *suc*2-Δ9	Robinson *et al.* (1988)
*vac14*Δ	SEY6210; *vac14*Δ*::TRP1*	Gary *et al.* (2002)
*vac14*Δ Fab1-Myc	SEY6210; *vac14*Δ*::TRP1 FAB1-Myc::HIS3*	Botelho et al.(2008)
Vac14-HA	SEY6210; *VAC14-HA::TRP1*	Botelho et al. (2008)

2.3 Plasmids

The full length *VAC14* gene in *S. cerevisiae* consists of 2640 base pairs. Truncated mutants of the *VAC14* gene have been previously isolated by Amra Saric and Danielle Taylor (Saric, 2009). A total of fourteen truncation mutants were isolated, six of which sequentially eliminate portions of the Vac14 protein from the C-terminus (VC1-C6) and eight that eliminate portions from the N-terminus (VN1-VN8). The full length, C-terminal and N-terminal truncated mutants of *VAC14* were previously amplified by polymerase chain reaction (PCR) and inserted in the yeast expression vector (pRB415A-FLAG) inside the multiple cloning site between the 5' BglII and 3'XhoI restriction sites (Figure 2.1). This vector contains an ampicillin resistence gene

(Amp^r) and leucine synthesis gene (*LEU2*). These two selectable markers permit the isolation of bacteria or yeast transformed with the plasmid by culturing on either ampicillin-containing media or leucine-deficient media. Moreover, the vector has an ADH promoter, and expresses two tandem copies of FLAG epitope on the 5' of the multiple cloning site (MCS) to generate N-terminal FLAG tagged protein for detection by anti-FLAG antibodies using Western blotting and immunoprecipitation (Saric, 2009).

T7-Vac14-His was obtained previously for recombinant protein expression, purification and in vitro binding (Botelho et al., 2008). In brief, *VAC14* was amplified by PCR and inserted into the bacterial expression vector, pET23d(+) between the 5' EcoRI and 3'XhoI restriction sites. The recombinant T7-Vac14-His has the T7 epitope and His_6 tag on the N-terminal and C-terminal ends of Vac14, respectively (Botelho et al., 2008). For the current study, T7-Vac14-His was used as a template DNA in site-directed mutagenesis to create Vac14 point mutants (details in section 2.10). The generated bacterial expression vector carrying Vac14 point mutants were expressed, purified and used for the *in vitro* binding assay (See Figure 4.1 in Chapter 4) (Ho, 2011).

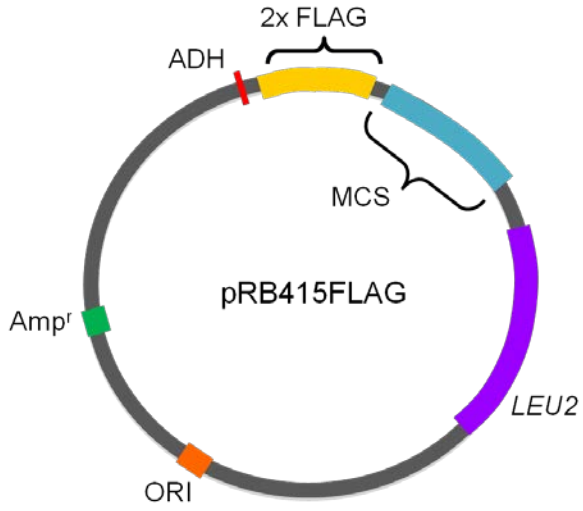

Figure 2.1 Simplified diagram of pRB415-FLAG. The plasmid vector contains the following: ADH: Alcohol dehydrogenase promoter (red), 2x FLAG: two tandem copies of FLAG epitope (yellow). MCS: multiple cloning site where *VAC14* gene is inserted (blue), *LEU*: Leucine gene (purple), Amp^r: ampicillin-resistance gene (green). ORI: replication origin for proliferation in the host cell (orange).

2.4 Bacterial transformation and DNA purification

One microliter of plasmid DNA was added to 50 µl of competent cells DH5α and incubated on ice for 30 min, followed by heat shock at 42 ºC for 45 seconds and immediately incubated on ice for 2 minutes. One milliliter of Luria-Bertani (LB) media was added to the transformation reaction. After incubation for 40-60 min at 37ºC, 250 µl of transformed cells were plated on LB-Amp plates (containing 100 µg/ml of ampicillin) followed by incubation at 37ºC overnight. All plasmid DNA in this study was isolated using EZ-10 spin column plasmid DNA kit (Bio-Basic INC) as described by manufacturer.

2.5 Yeast transformation

Transformation of plasmid DNA into the appropriate yeast strain was conducted as follows: single colony of yeast cells was inoculated into 5 ml of the Yeast Peptone Dextrose (YPD) at 26 ºC with constant shaking at 250 rpm overnight. Yeast cultures were then diluted to OD_{600} of 0.100 and grown to OD_{600} of ≈ 0.6 on 1.5 ml of the yeast culture was centrifuged at 12,000 rpm for 1 min. The pellet was washed with 0.1 M lithium acetate (LiAcTE), and resuspended into 300 µl of 40% Polyethylene glycol (PEG) and LiAcTE. Plasmid DNA (≈1 µg) and 10 µl of 5 mg/ml salmon sperm DNA, which has been boiled 5 min, were added to the 40 % PEG LiAcTE, followed by incubation for 1 hour at room temperature. The transformation mixture was treated with 10% of dimethyl sulfoxide (DMSO) and heat shocked at 42 ºC for 10 min and subsequently for 2 min on ice. Cells were centrifuged at 12,000 rpm, resuspended in 150 µl of sterile water, plated on the appropriate selective media (SD-leucine) and incubated at 30 ºC for 3 days.

2.6 Whole cell lysates

A single colony of yeast cells was inoculated in 3 ml of selective SD media as appropriate and grown with shaking overnight at 30ºC. The overnight culture was transferred to 5 ml SD media as required to a final OD_{600} of 0.15 and grown with shaking at 30ºC to a final OD_{600} of ≈0.6. Cells were collected at 2500 rpm for 5 min and re-suspended in 1 ml cold deionized water, followed by spinning down for 2 min at 12000 rpm at room temperature and resuspended again in 1 ml cold deionized water. Ten percent of cold trichloroacetic acid (TCA) were added to precipitate protein on ice for at least 30 min. After centrifugation at 14000 rpm for 3 min, the pellet was resuspended in 1 ml of cold acetone and sonicated in an ultrasonic bath until completely resuspended. The cell pellet was dried, followed by resuspension in sample buffer (100 mM Tris, pH 6.8, 4% SDS, 10% glycerol, 1% bromopheno blue, and 10% 2-mercaptoethanol). One scoop (≈ 100 µl) of glass beads were added to the sample buffer, followed by vortex for 5 min at maximum speed and boiled for 5 min for protein extraction. Protein expression was assessed through SDS-PAGE and Western blotting.

2.7 Co-immunoprecipitation (CoIP)

Yeast cultures (25-100 ml) were grown overnight in appropriate media to an OD_{600} of ≈ 0.6. Cells were centrifuged for 5 min at 4000 rpm at 4ºC. Pellets were re-suspended at 5 ODs/ml in 100 mM Tris pH 9.4 with 10 mM dithiothreitol (DTT) added fresh, followed by incubation at room temperature for 10 min. Cells were collected at 4000 rpm for 5 min and re-suspended in spheroplasting media (2% glucose**,** 1 X amino acids**,** 1 M sorbitol**,** 20 mM Tris pH 7.5**,** 1X YNB). Five microliters of 10 mg/ml zymolase stock (GBBiosciences) were added per OD_{600} of cells (7-15 mg/ OD_{600} unit of cells). Cell wall digestion was done with continuous shaking at

30ºC. Loss of cell wall was confirmed by 1/100 diluting in water OD_{600} approximated zero. Spheroblasted cells were washed in 1 ml ice-cold spheroblasting buffer and lysed in a 2-ml Dounce homogenizer in 1 ml HEPES-lysis buffer (20 mM HEPES, pH 7.2, 50 mM potassium acetate, 200 mM sorbitol, and 2 mM EDTA), supplemented with 3X complete protease inhibitor cocktail, 0.3 mM 4-(2-aminoethyl) benzenesulfonyl fluoride, 3 mM benzamide. Unbroken cells were removed by centrifugation at 2000 rpm for 10 min. Cell lysates were solublized with Tween-20 with a final concentration of 0.25%, rotating at 4ºC for 15 min. Detergent-insoluble material was spun down at 13,000 xg for 10 min. The supernatant was collected and spun down again at 13,000 g for 5 min. Twenty percent of the volume was used as input, mixed with 10% TCA, incubated for 1 hr on ice, sonicated with acetone and processed with Laemmli buffer. Immunoprecipitation (IP) was performed by adding 1 µg/ml of monoclonal antibodies, anti-FLAG antibodies (M2; Sigma-Aldrich) rotating for 1 hour at 4ºC. About 200 µl of GammaBind G-linked Sepharose beads (GE Healthcare) were added rotating for 1–2 h at 4ºC. Beads were washed three times with HEPES-lysis buffer containing 0.25% Tween 20 and two times without detergent. Bound proteins were extracted with 2X sample buffer and heated at 95ºC for 5 min, removed from the beads with a loading tip into a new eppendorf tube, followed by SDS-PAGE and Western blotting for analysis.

2.8 SDS-Polyacrylamide Gel (PAGE) and Western Blotting

All samples obtained from yeast cell lysates and coIPs were loaded onto a 5% stacking and 9% separating SDS-polyacrylamide gels and immersed into 1 X Tris/SDS running buffer (Biobasic Ltd.). An electric field of 130 V was applied for 20 min and then increased to 160

Volts for protein separation. Protein standards containing reference bands (Bio-RAD) were used to facilitate assessment of relative protein sizes.

SDS-PAGE was followed by Western blotting in which separated proteins where transferred onto polyvinylidene fluoride membranes activated with methanol (BioTrace^{TM}PVDF, PALL Corporation, Life Sciences) at 100 V for 1 hour in 1X Tris /Glycine transfer buffer (Biobasic Ltd.). Membranes were then blocked for one hour at room temperature in 1X Tris buffered saline (TBS); (20 mM Tris, 150 mM NaCl, 2 mM KCl, pH 7.4) with 0.05% Tween-20 (TBST) and 5% fat free skim milk. After blocking, primary antibodies were added at appropriate dilutions in TBST. Monoclonal anti-FLAG antibodies (M2; Sigma-Aldrich) were used at 1:2500 dilutions. Monoclonal anti-HA antibodies (Abcam) were used at 1:2000 dilutions. Monoclonal anti-Myc antibodies (Bioshop) were used at 1:1500 dilutions. Fig4 was detected with rabbit anti-Fig4 polyclonal antibodies at a concentration of 1:20000. Membranes were probed with primary antibodies overnight at 4ºC. The following day, blots were washed 4 times with 1X TBST for 15 min to remove non-specific binding. Horseradish peroxidise (HRP)-linked secondary anti-mouse antibodies (1:5000), or HRPO goat anti-rabbit IgG (H+L)(1:25000) were then added in TBST with 5% skim milk and incubated for 1 hr at room temperature. Two milliliters of Immun-Star WesternC Chemiluminescent solution (BioRad) or ECL (GE healthcare) were added to the blots and incubated for 5 min for Chemiluminescent signal generation. The excess solution was drained from blots and then placed on a piece of Saran Wrap and exposed to chemiluminescence film (GE Healthcare Ltd.) for 30 sec up to 5 min. To visualize proteins, the film was developed using GBX developer and fixed using GBX fixer (Kodak, Rochester, NY, USA).

2.9 Bioinformatics

Multiple alignments between the protein sequence of yeast Vac14 and Vac14 orthologs from other eukaryotic species was performed using ClustalW2. The purpose of this alignment was to highlight the most conserved motifs in the C-terminus of Vac14. These motifs were then selected to target Vac14 point mutations. Geneious Pro 5.4.4, software used for DNA and protein sequence analysis was also utilized for aligning sequences of Vac14 point mutants with wild-type of *VAC14* to confirm successful mutagenesis.

The amino acid sequence in the C-terminal region of Vac14 was scanned for HEAT repeats using the repeat finding program, REP (http://www.embl.de/~andrade/papers/rep/search.html) (Jin et al., 2008).

2.10 Construction of v*ac14* point mutants by site-directed mutagenesis

Methylated pET23d(+)T7-Vac14-His plasmid was used as template DNA to create point mutations in full length of *VAC14* using the QuikChange II XL site-directed mutagenesis kit according to manufacturer instructions (Agilent Technologies). Linear amplification of the plasmid was performed using *PfuUltra* high-fidelity (HF) DNA polymerase and two complementary synthetic oligonucleotide primers that both contained the desired mutations. Parental DNA lacking mutations was digested with the methylated DNA directed enzyme *DpnI*. Six oligonucleotide primers were designed as described in the table below:

Table 2.2 Designed oligonucleotides used as primers to create v*ac14* point mutants in site-directed mutagenesis.

Mutant name	Name of 5' oligo	Sequence of F oligo	Name of R oligo	Sequence of 3' oligo	Position of mutated nucleotide on *VAC14* ORF	Mutated nucleotide	Mutated amino acid residue	Position of mutated amino acid residue
vac14 ^{560SS}	Vac14-560SS-F	5'CGTCAGTCTCTTCAAGATTCATTAACTTTA 3'	Vac14-560SS-R	5'TAAAGTTAATGAATCTTGAAGAGACTGACG 3'	1679	TTA to TCT	Phenylalanine (F) to Serine (S)	560
					1691	TTA to TCA	Lysine (L) to Serine (S)	564
vac14 ^{582NG}	Vac14-582NG-F	5'GCAAACTTTAACATGGGACAGATATCT 3'	Vac14-582NG-R	5'AGATATCTGTCCCATGTTAAAGTTTGC 3'	1746	ATC to AAC	Isoleucine (I) to Asparagine (N)	582
					1751	AGA to GGA	Arginine (A) to Glycine (G)	584
vac14 ^{623SIA}	Vac14-623SIA-F	5'ACAAACTCAATAATTTCACCGGCGATGTCG 3'	Vac14-623SIA-R	5'CGACATCGCCCGGTGAAATTATTGAGTTTGT 3'	1868	TTA to TCA	Lysine (L) to Serine (S)	623
					1874	ACT to ATT	Threonine (T) to Isoleucine (I)	625
					1883	GAG to GCG	Glutamic acid (E) to Alanine (A)	628
vac14 ^{651CRY}	Vac14-651CRY-F	5'TTATTCAAATGTCGGTATCCCAACCCC 3'	Vac14-651CRY-R	5'GGGGTTGGGATACCGACATTTGAATAA 3'	1952	TCT to TGT	Serine (S) to Cysteine (C)	651
					1945	TGG to CGG	Tryptophan (W) to Arginine (R)	652
					1958	TGT to TAT	Cysteine (C) to Tyrosine (Y)	653
vac14 ^{661AES}	Vac14-661AES-F	5'TCCGTGATAGCCGAATCTTTTGTAGCAGAA3'	Vac14-661AES-R	5'TTCTGCTACAAAAGATTCGGCTATCACGGA3'	1981	TCC to GCC	Serine (S) to Alanine (A)	661
					1984	TTA to GAA	Leucine (L) to Glutamic acid (E)	662
					1985	TGT to TCT	Cysteine (C) to Serine (S)	663
					1988			
vac14 ^{729TRE}	Vac14-729TRE-F	5'ATACTGACGATTATACGAGAGTCAAAGGCA3'	Vac14-729TRE-R	5'TGCCTTTGACTCTCGTATAATCGTCAGTAT3'	2186	ATG to ACG	Methionine (M) to Therionine(T)	729
					2195	CCA to CGA	Proline (P) to Arginine (R)	732
					2197	CAG to GAG	Glutamine (Q) to Glutamic acid (E)	733

Using the reagents provided with mutagenesis kit (QuickChange® II XL Sit-Directed Mutagenesis Kit, Agilent Stratagene), sample reactions were prepared. Each reaction consisted of 5 µl of 10X reaction buffer, 40 ng of DNA template (pET23d(+)-T7-Vac14-His), 125 ng of forward oligonucleotide primer, 125 ng of reverse oligonucleotide primer, 1µl of dNTP mix, 3 µl of QuickSolution, and deionoized water to a final volume of 50µl. One microliter of *PfuUltra* HF DNA polymerase (2.5 U/µl) was added after setting the thermal cycler at 95ºC for 2 min. The thermal cycler was used using recommended cycling parameters outlined in the mutagenesis kit manual with slight modifications as following:

Table 2.3 Thermal cycling settings used for site-directed mutagenesis

Segment	Cycles	Temperature	Time
1	1	95ºC	2 min
2	25	95ºC	1 min
		35ºC	50 sec
		68ºC	10 min
3	1	68ºC	7 min

Following amplification, the reactions were digested with 1µl of *Dpn* I (10 U/µl) restriction enzyme to digest parental DNA and incubated at 37ºC for 1-2 hr. *Dpn* I-treated DNA was transformed into the bacterial strain, XL10-Gold ultracompetent cells provided with the mutagenesis kit. Bacterial transformation was followed as described by the manufacturer. The grown colonies were isolated and DNA was extracted with EZ-10 spin column plasmid DNA kit (Bio-Basic INC).

2.11 Sequencing

All samples for DNA sequencing were prepared by adding 250 ng of plasmid miniprep DNA and 7 pmol of sequencing primer mixed with water to give a total of 7.7µl. DNA sequencing was conducted on the following clones:

A. Bacterial version of Vac14 point mutants
   - pET23d(+) T7- *vac14*^{560SS}-his
   - pET23d(+) T7-*vac14*^{582NG}-His
   - pET23d(+) T7- *vac14*^{623SIA}-His
   - pET23d(+) T7- *vac14*^{651CRY}-His
   - pET23d(+) T7- *vac14*^{661AES}-His
   - pET23d(+) T7- *vac14*^{729TRE}-His

B. Yeast version of Vac14 point mutants
   - pRB415-FLAG- *vac14*^{560SS}
   - pRB415-FLAG- v*ac14*^{582NG}
   - pRB415-FLAG- *vac14*^{623SIA}
   - pRB415-FLAG- *vac14*^{651CRY}

Vac14-R2100 primer was used to sequence near base pair 2100 of *VAC14* in the reverse direction. Different primers were used to sequence the entire *VAC14* including Vac14-R1100, Vac14-R1700, which reverse sequences at base pairs 1100 and 1700, respectively; T7, and T7-terminator primers, which anneal to specific sequences outside the MCS of the plasmid toward the gene of interest, were used to sequence 5' and 3' ends of *VAC14*. Samples were sent to The Centre for Applied Genomic DNA Sequencing Facility at MARS building in Toronto.

2.12 Cloning of Vac14 point mutants into the yeast expression vector

The generated pET versions of Vac14 point mutants including *vac14*^{560SS}, *vac14*^{582NG}, *vac14*^{623SIA} and *vac14*^{651CRY}, were PCR amplified using previously designed primers containing BglI and XhoI restriction sites for cloning full length of *VAC14.* Amplified products were seperated on 0.8% agarose gel electrophoresis to confirm yield of the amplified *VAC14* point mutants of approximate size 2.6 kilobase (kb). The PCR products were purified using an EZ-10 Cleanup Kit (Bio-Basic Ltd). The yeast expression vector, pRB415A-FLAG, and the amplified Vac14 point mutants were digested with BglII and XhoI restriction enzymes at 37ºC for 2 hr. Alkalaine phosphatase was added to the vector on the second hour of the incubation with the restriction enzymes. The digestion mixtures were cleaned up and each amplified mutant was ligated into pRB415A-FLAG using T4 DNA ligase (New England Biolabs) at 16 ºC overnight. Ligated products were transformed into DH5α and plasmid DNA was purified from single colony as outlined previously and sent for sequencing to confirm mutation.

2.13 Fluorescence labeling of vacuoles and fluorescence microscopy

One milliliter and a half of SD culture of yeast cells (OD_{600} of ≈ 0.6) was centrifuged at 12,000 rpm for 2 min. Supernatant was aspirated and cells were resuspended in 100 µl of the remaining media. Vacuoles were labeled with 100 nM of 4-chloromethyl-7-aminocoumarin (CMAC) for 10 min. Subsequently, cells were resuspended in 25-50 µl fresh SD media. Fluorescence and differential interference contrast (DIC) images of labeled cells were obtained with a Leica DM5000B compound upright microscope (Leica Microsystems, Canada). Background intensity levels were linearly adjusted using Adobe Photoshop CS5 (Adobe Systems, San Jose, CA).

3 Results

3.1 Expression of Vac14 truncated mutants in yeast

The first step in evaluating the function of the Vac14 self-interaction was to analyze the Vac14 self-interaction region. The *VAC14* mutants containing sequential deletions of *VAC14* were used to determine the most disruptive region of truncation of Vac14 that is simultaneously unable to interact with wild type Vac14. Consequently, the shortest mutant of Vac14 that is able to maintain the interaction with wild type Vac14 can be a potential region for Vac14-self interaction. Deletion mutants were derived from full length *VAC14* that was truncated sequentially from C-terminus and N-terminus and inserted into pRB415A-FLAG as outlined previously in Chapter 2. A total of six C-terminal truncations and eight N-terminal truncations were generated (Figure 3.1 and 3.2). The strategy for designing these mutants was to sequentially delete either portions or the entire conserved HEAT repeats from both ends of Vac14. Wild type Vac14 was also inserted into pRB415A-FLAG and used as a positive control for Vac14 expression and self-interaction. Each truncated mutant was transformed into Vac14-HA, a wild-type strain with the chromosomal *VAC14* tagged with HA. Whole cell lysates from Vac14-HA expressing FLAG-tagged Vac14 truncated mutants were obtained, followed by SDS-PAGE and Western blotting to test their expression. The expected molecular weight sizes of the Vac14 truncations were calculated (Table 3.1), and compared with the sizes of the expressed truncated mutants (Figure 3.3).

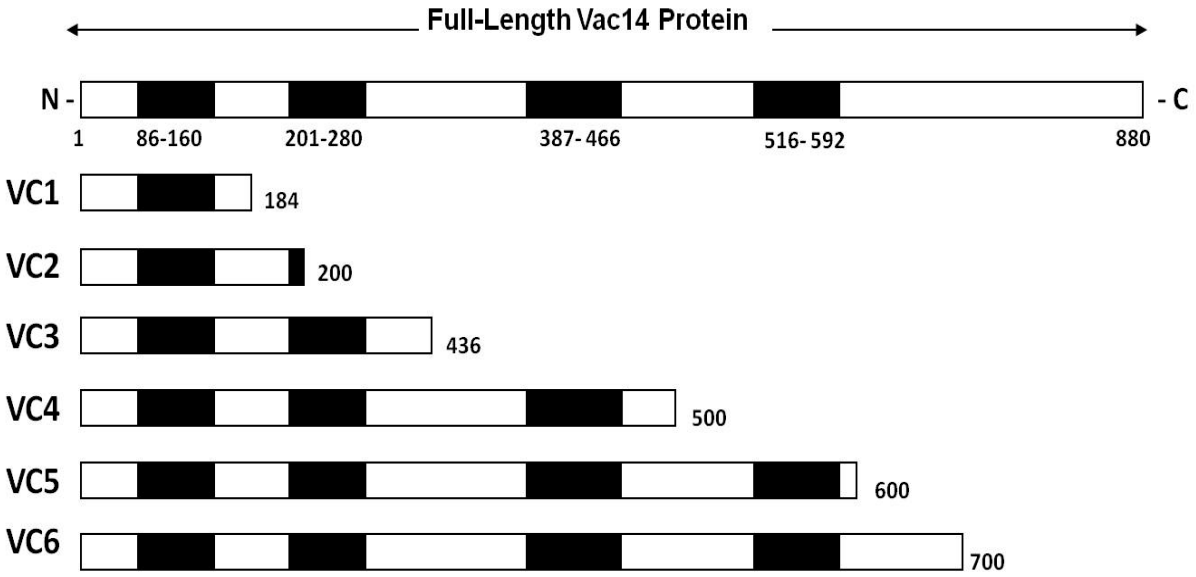

Figure 3.1. Schematic representation of C-terminus truncations of Vac14. Full length Vac14 protein consists of 880 amino acids. Each truncated mutant has a different length as a result of sequential deletion of the indicated residues from the C-terminus. The name of each mutant is shown on the left (VC1 to VC6). The mutant residue number is shown on the far right. The predicted high-confidence HEAT repeats of Vac14 are shown in black.

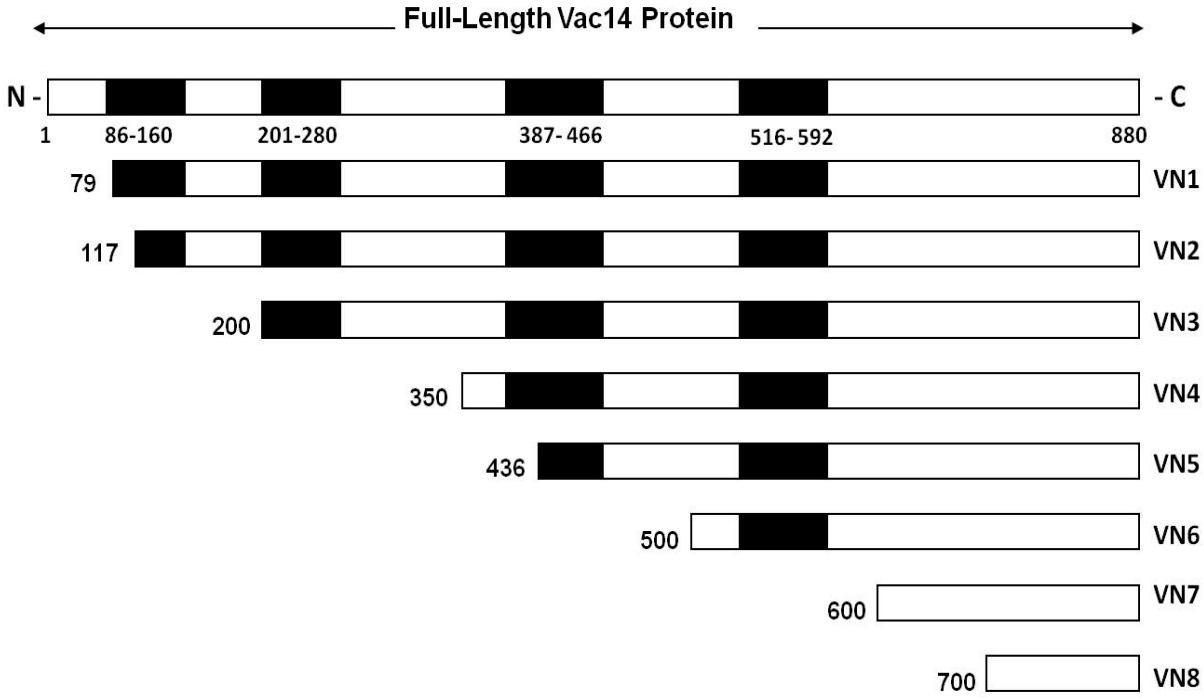

Figure 3.2. Schematic representation of N-terminus truncations of Vac14. Truncated mutants from the N-terminus include 8 mutants that have different lengths as a result of sequential deletions of the indicated residues from the N-terminus. The name of each mutant is shown on the right (VN1 to VN8). The mutant residue number is shown on the left. Predicted high-confidence HEAT repeats of Vac14 are shown in black.

Table 3.1 Expected molecular weight of Vac14 truncations

N-terminus truncations	MW (kDa)	C-terminus truncations	MW (kDa)
VN1	91	VC1	20.38
VN2	86.7	VC2	29
VN3	77.48	VC3	37.54
VN4	60.56	VC4	49.95
VN5	50.92	VC5	67.49
VN6	44	VC6	79
VN7	32.29	----	----
VN8	20.71	----	----

- Vac14 full length ≈ 100 kDa

Western blot analysis demonstrated successful expression for some of the Vac14 truncated mutants including VC3, VC4, VC5 and VC6 for C-terminal truncations, and VN3, VN4, VN5, VN6 for N-terminal truncations, respectively (Figure 3.3). VC1 and VC2 were not detected, which may have been lost as a result of the gel being run for too long. The N-terminal truncations, VN7 and VN8, may have been undetected for similar reasons. Moreover, VN1 and VN2 seem to overlap with non-specific bands. Thus, it is uncertain if these truncations are expressing or not. To estimate the Vac14 self-interaction region, we conducted coIP between the expressed truncated mutants and full length Vac14.

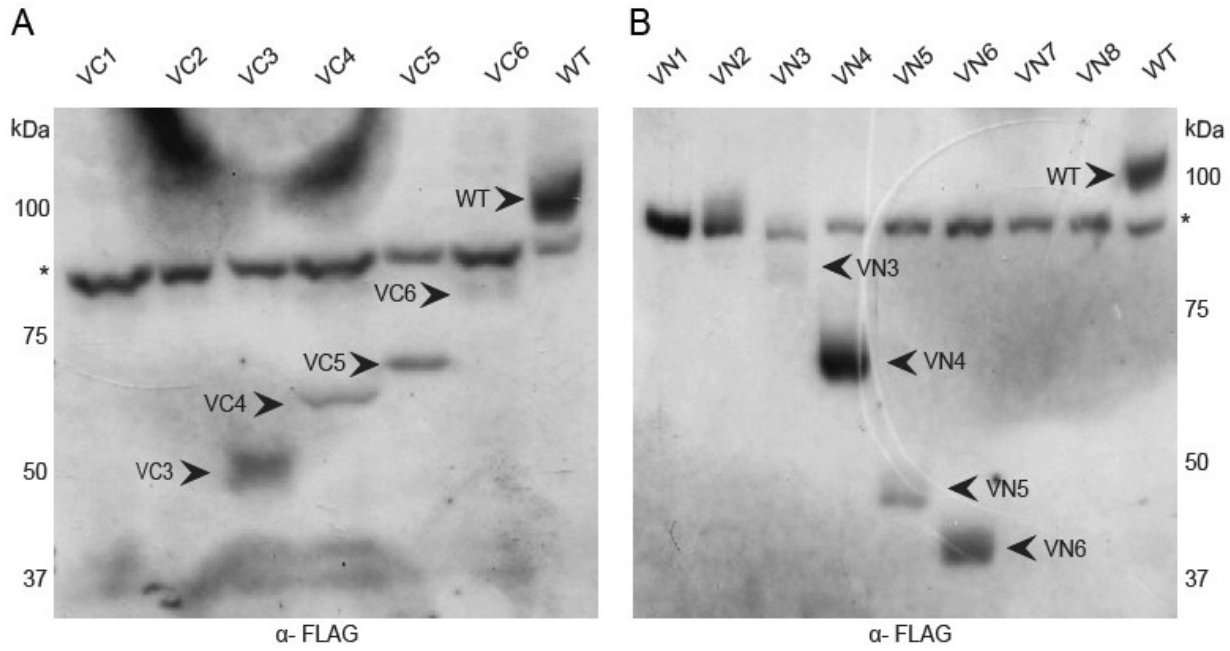

Figure 3.3 Protein expression of C-terminus and N-terminus truncated mutants of Vac14 in yeast. Whole cell lysates from cells expressing wild type Vac14-FLAG (WT), C-terminal (A) and N-terminal (B) truncated mutants were obtained, followed by SDS-PAGE and Western blot using anti-FLAG antibodies for detection. An * (asterisk) indicates non-specific bands detected by anti-FLAG antibodies.

3.2 The C-terminal region of Vac14 is required for self-interaction

CoIP is one of the most practical techniques used to identify protein-protein interaction from a whole cell lysate. The principle is based on precipitating the protein of interest in its native form using antibodies against the native protein or a fused epitope tag and detecting any other associated proteins (Anderson, 1998). In the current study, the key experiment was to test which Vac14 truncation failed to co-precipitate wild type Vac14-HA after IP with anti-FLAG antibodies in order to estimate the self-interaction region. Briefly, yeast cells expressing Vac14-HA and a FLAG-tagged Vac14 truncation are incubated with anti-FLAG antibodies and Protein G-linked beads. The one possible scenario, wild type Vac14-HA co-immunoprecipitates with a FLAG-tagged Vac14 truncation, indicating that they interact and the eliminated portion for the tested mutant did not affect the self-interaction (Figure 3.4.A). The second scenario, the

truncated mutant fails to coIP with Vac14-HA, indicating that they do not interact and suggesting that the truncated region of Vac14 is essential for self-interaction (Figure 3.4.B). Detection of the interaction region was then assessed by Western bloting in order to detect whether or not Vac14-HA is recovered with immunoprecipitation of FLAG-tagged Vac14 truncations.

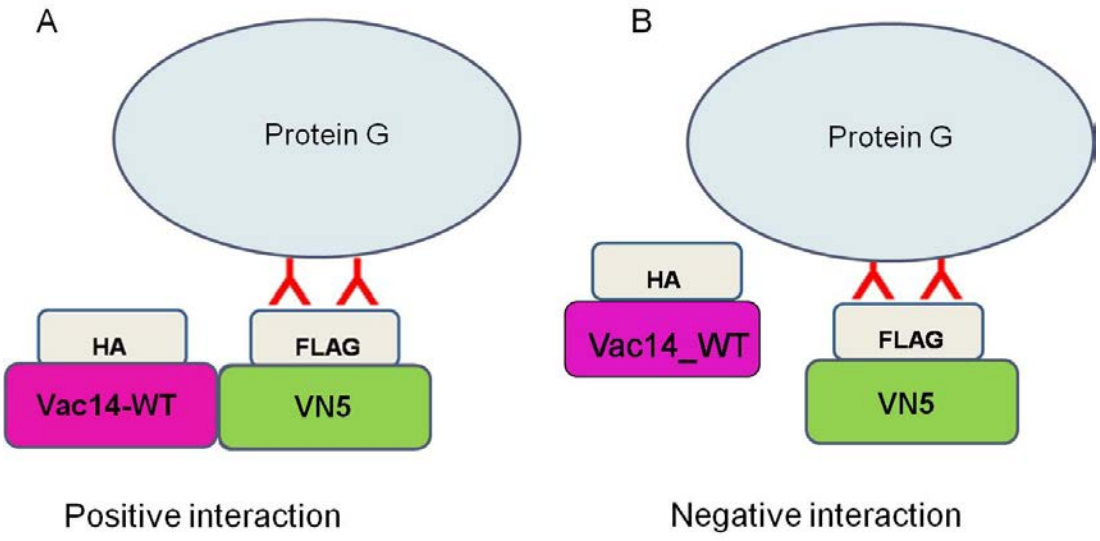

Figure 3.4. Model for co-immunopreciptation of wild type Vac14-HA with Vac14 truncated mutant. A. Vac14-HA interacts with the truncated mutant.VN5 is used as an example of the mutants. The positive interaction is revealed by immunopreciptation with anti-FLAG antibodies are then captured on GammaBind G, sepharose beads linked to a recombinant form of streptococcal protein G. **B.** Negative interaction involves precipitating the FLAG-tagged VN5 only, and Vac14-HA is not co-precipitated. Anti-FLAG antibodies bind only to VN5 and Vac14-HA is not recovered.

First, coIP between N-terminal Vac14 truncations and Vac14-HA was performed (Figure 3.5). To confirm Vac14-self interaction, lysates from cells expressingVac14-HA transformed with wild type Vac14-FLAG were obtained to test for coIP. Our results showed that IP of wild type Vac14-FLAG recovered Vac14-HA and this was used as a positive control for Vac14 self-interaction. However, lystates from cells expressing Vac14-HA alone, which lack the FLAG epitope, were used as a negative control to ensure the specificity of anti-FLAG antibodies

First, coIP analysis was performed to test the interaction of N-terminal truncations with Vac14-HA. The first blot was probed with anti-FLAG antibodies to confirm IP of wild type Vac14-FLAG and FLAG-tagged Vac14 truncations. Input lanes represent 20% of the total material used to confirm the expression of the controls and the truncated mutants. IP with anti-FLAG antibodies from whole cell lysates expressing FLAG-tagged VN4 and VN5 were successfully pulled down (Figure 3.5). However, VN5 seemed to overlap with IgG heavy chain as it has similar molecular weight ≈ 50 kDa. The second blot was probed with anti-HA antibodies, to see whether Vac14-HA is co-immunoprecipitated with FLAG-tagged Vac14 truncations. A significant amount of Vac14-HA was recovered with VN4, which suggests that deleting the first 350 residues from the N-terminus of Vac14 did not disrupt self-interaction. In contrast, VN5 in which 436 residues were truncated showed significant reduction of Vac14-HA, suggesting that residues 346 to 436 stabilize Vac14 self-interaction.

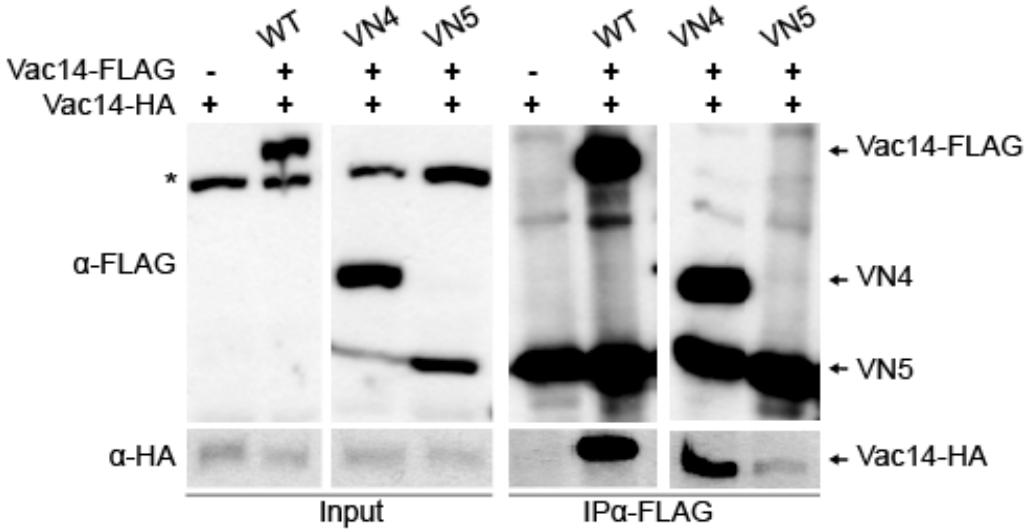

Figure 3.5. N-terminus truncated mutants interact with Vac14. IPs were done with monoclonal anti-FLAG from whole cell lysates from wild type Vac14-FLAG, VN4 and VN5 with Vac14-HA. Input lanes represent 20% of total protein used for the IP experiment. Vac14-HA was used as a negative control to ensure the specifity of each co-IP. The blots were probed as indicated. Western blotting with anti-FLAG antibodies was used to confirm immunoprecipitation of Vac14 truncated mutants and wild type Vac14-FLAG. Western blotting with Anti-HA antibodies was used to detect whether Vac14-HA was recovered.

To further estimate the Vac14 self-interaction region, another coIP was performed to see if the C-terminus of Vac14 could be a potential region for the self-interaction. The coIP analysis suggested that in the C-terminus truncated mutant VC5 disrupts the interaction with Vac14-HA, suggesting that amino acid residues 500 to 880 in Vac14 are crucial for the self-interaction (Figure 3.6). By comparison, the N-terminal truncated mutants including VN4 and VN5 did not entirely fail to interact with Vac14-HA comparing to VC5, suggesting that the amino acid residues 500 to 880 in the C-terminus are required for Vac14 multimerization.

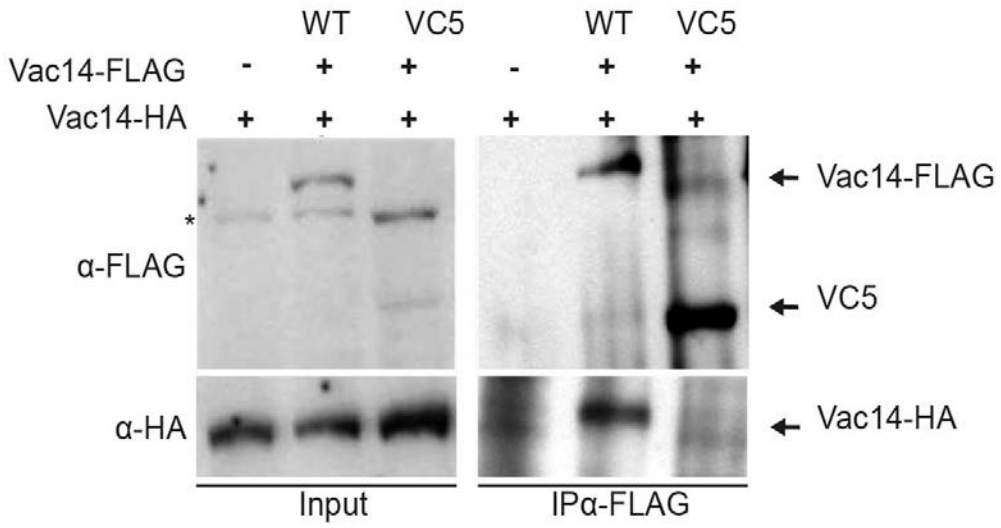

Figure 3.6. VC5, a C-terminus truncated mutant failed to interact with Vac14. IPs were done with monoclonal anti-FLAG antibodies from whole cell lysates from wild type Vac14-FLAG, VC5 with HA-tagged Vac14. Input lanes represent 20% of total protein used for the IP experiment. Anti-FLAG were used in the first blot to confirm immunoprecipitation of Vac14 truncated mutants and wild type Vac14-FLAG. Anti-HA antibodies were used to detect whether Vac14-HA was recovered.

After several attempts to estimate the potential region for Vac14 self-interaction, we propose that the self-interaction domain is between 500 to 800 amino acids sequence in the C-terminus of Vac14 protein.

3.3 Point mutant design in the C-terminus of Vac14

After estimating the Vac14 self-interaction region, we focused on identifying the motifs responsible for the interaction within the C-terminus of Vac14. Point mutations were made in the most conserved motifs in the C-terminus of Vac14 to determine which motifs might be responsible for self-interaction. The conserved motifs were identified by alignment of Vac14 ortholog sequences from different species using ClustalW. Six highly conserved motifs were identified in the C-terminal Vac14. Only four of the highly conserved motifs are shown (Figure 3.7). The other two conserved motifs are located in between residues 660 to 664 and 724 to 737, respectively. Based on this, six DNA primers were designed to introduce disruptive point mutations in these six motifs by site-directed mutagenesis. Our strategy for creating these mutations was to change the properties of two or three selected conserved residues in each motif. For example, an amino acid with a hydrophobic side chain such as phenylalanine was mutated to an amino acid with a polar uncharged side chain such as serine. Using the pET23::*VAC14* encoding a recombinant wild-type Vac14 (T7-Vac14-HIS) as a template, the designed primers were used to generate the point mutations in T7-Vac14-HIS by site-directed mutagenesis. Miniprep DNA of various clones were isolated and sent for sequencing to confirm expected mutations by alignment with wild type Vac14 (Figure 3.8).

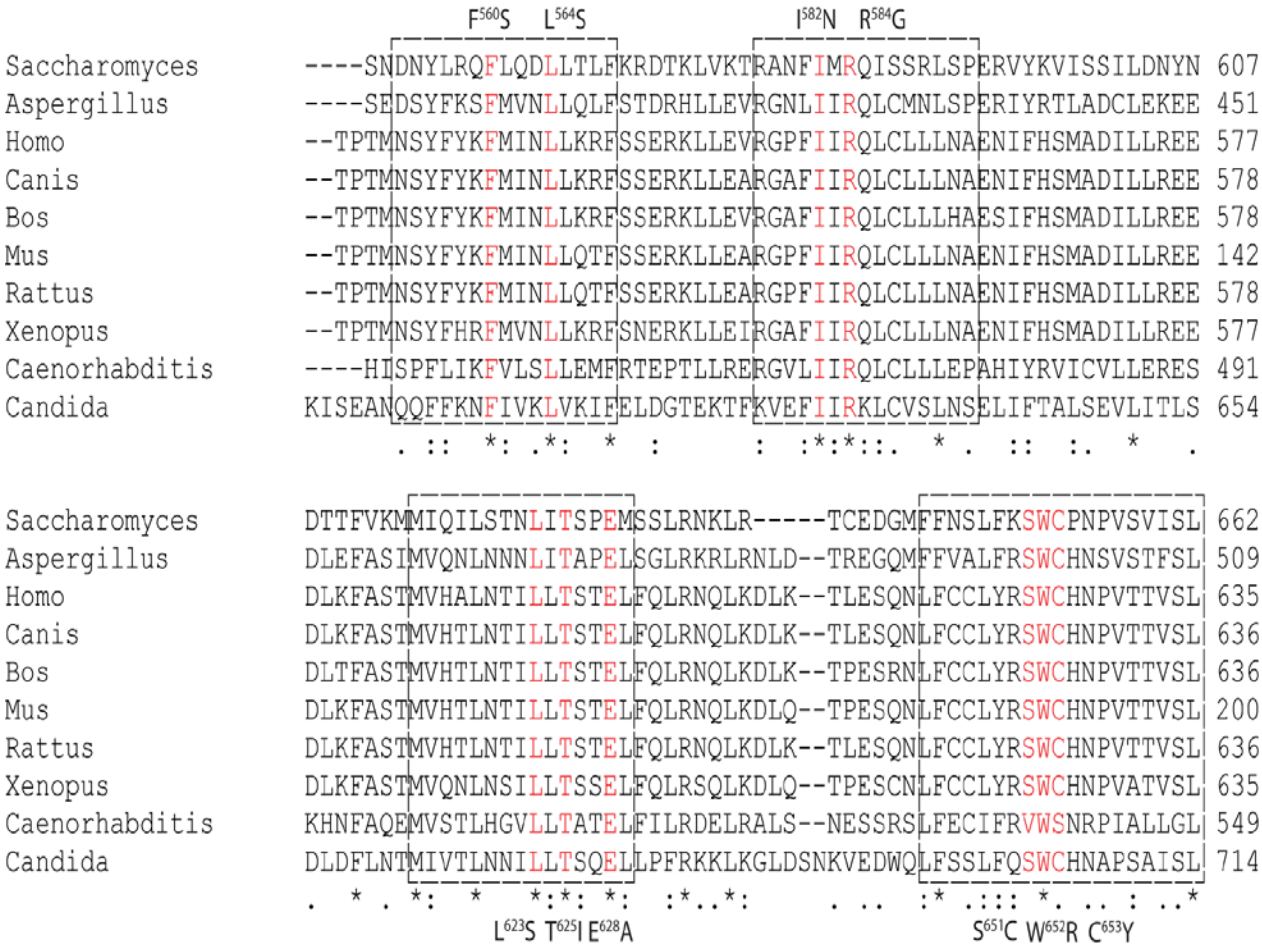

Figure 3.7. Multiple alignment of Vac14 amino acid sequence in yeast and from other eukaryotic species. Highlighted regions represent the selected conserved amino acids selected for site-directed mutagenesis of Vac14. "*" (asterisk) indicates positions which have a single, fully conserved residue. ": "(colon) indicates conservation between groups of strongly similar properties. "." (period) indicates conservation between groups of weakly similar properties.

Four of the six point mutants were successfully cloned (Figure 3.8). The four obtained Vac14 point mutants included *vac14*^{SS}, *vac14*^{SIA}, *vac14*^{CRY} and *vac14*^{NG}, named according to the mutated amino acid residues (Figure 3.9).

Figure 3.8. Sequence alignment of Vac14 point mutants and wild-type Vac14 sequences. The dotted boxes indicate the mutated codon amino acids. Base and residue numbers are shown on the top of each sequence.

As described in Chapter 2.12, the Vac14 point mutants were amplified by PCR, digested and ligated into the yeast expression vector, pRB415A-FLAG. Yeast expression vectors carrying wild type Vac14 and Vac14 point mutants were transformed into the Vac14-HA yeast strain to test for expression, followed by coIP to test for the self-interaction.

3.4 Expression of Vac14 point mutants in yeast

To test the interaction of Vac14 point mutants with wild type Vac14-HA, we first estimated the steady-state expression levels of the FLAG-tagged Vac14 point mutants as compared to control wild type Vac14-FLAG. Expression of Vac14-HA was also tested to ensure equal expression levels in Vac14 point mutants and wild type Vac14. To this end, whole cell lysates were obtained from yeast expressing Vac14 point mutants or wild type Vac14-FLAG, followed by SDS-PAGE and Western blotting. All Vac14 point mutants were expressed including

Vac14^{560SS}, *Vac14*^{623SIA}, *Vac14*^{651CRY} and *Vac14*^{582NG}. *Vac14*^{560SS} and *Vac14*^{582NG} were expressed at similar levels as wild type Vac14. However, *Vac14*^{623SIA} and *Vac14*^{651CRY} appeared to be expressed at lower levels (Figure 3.10).

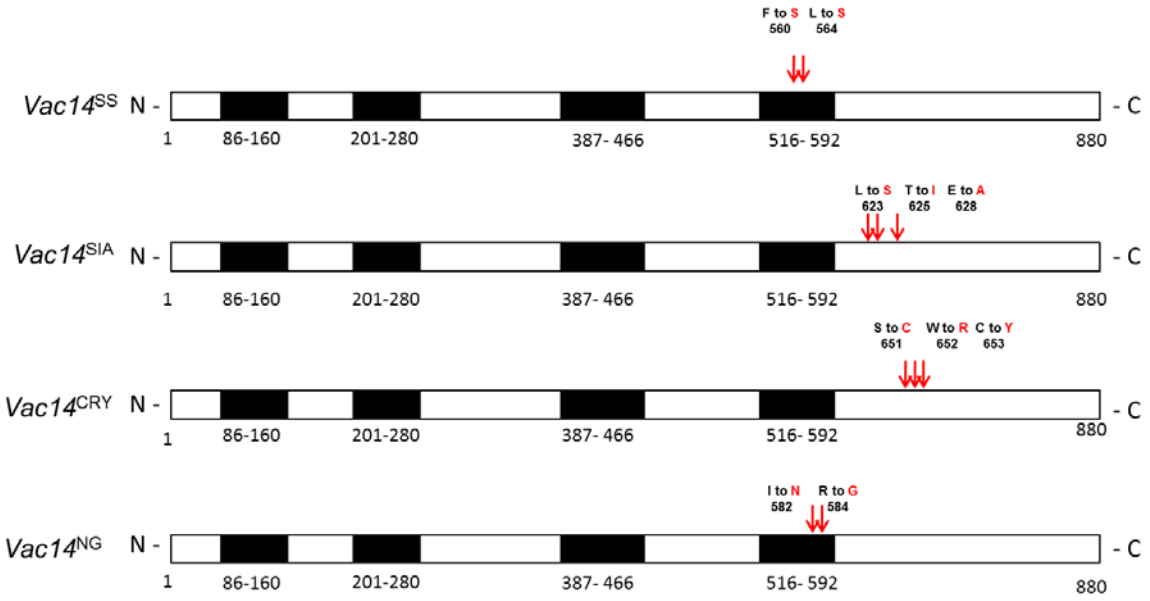

Figure 3.9. Schematic representation of Vac14 point mutants: Red arrows show the positions of the point mutations in Vac14. The wild type amino acid residue position is shown in black. The mutated amino acids are shown in red. For example, F to S refers to mutation from phenylalanine (F) to serine (S).

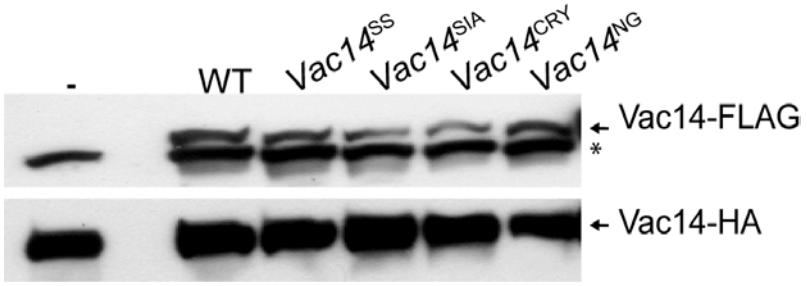

Figure 3.10. Protein expression of FLAG-tagged Vac14 point mutants in yeast. Whole cell lysate from Vac14-HA (-), Vac14-HA expressing wild type Vac14-FLAG (WT), and Vac14 point mutants were obtained, followed by SDS-PAGE and western blotting. Monoclonal anti-FLAG antibodies were used to detect the FLAG-tagged mutants. Vac14 point mutants including *vac14*^{560SS}, *vac14*^{623SIA}, *vac14*^{651CRY} and *vac14*^{582NG} are expressed (top). Monoclonal anti-HA antibodies were used to detect the expression level of chromosomal Vac14-HA (bottom). An * (asterisk) indicates non-specific bands.

3.5 Vac14 point mutants in the C-terminal motifs disrupt Vac14 self-interaction

To determine the specific motifs responsible for Vac14-self interaction, coIP was performed to test for interaction of the expressed FLAG-tagged Vac14 point mutants with Vac14-HA (Figure 3.11). Unlike wild type Vac14-FLAG, Vac14 point mutants showed significance loss of interaction with Vac14-HA. Based on visual estimation, *Vac14*^{SS} and *Vac14*^{CRY} point mutants abolished ~90% of the Vac14 self-interaction, and ~70% and ~50% with *Vac14*^{NG} and *Vac14*^{SIA} point mutants, respectively. This suggested that the mutated motifs in the C-terminus of Vac14 are potential sites for Vac14-self interaction. This also indicates that Vac14 mutants are monomeric.

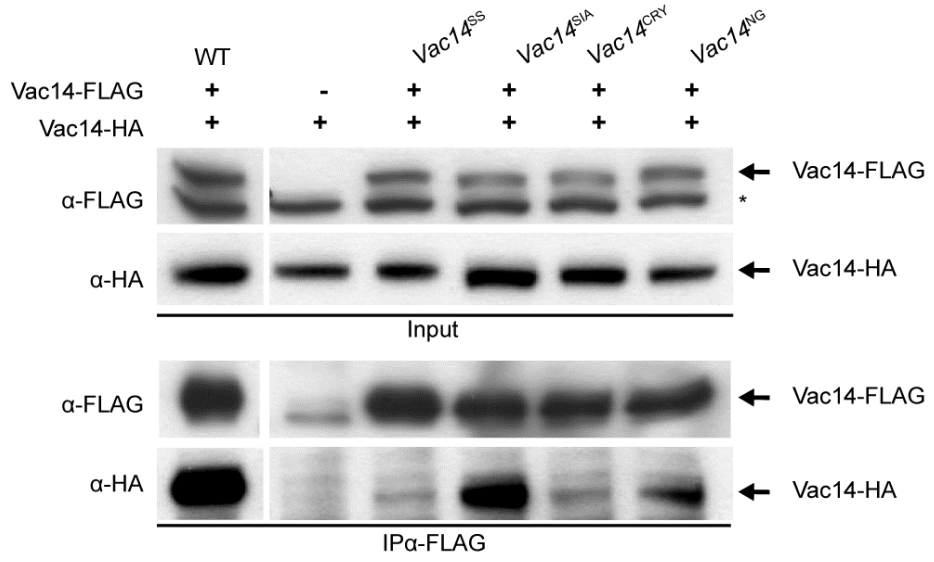

Figure 3.11. Vac14 point mutants disrupt Vac14 self-interaction. Input lanes represent 20% of total protein used for the IP experiment. Whole cell lysates were obtained from cells expressing Vac14-HA and transformed with empty vector (-), or with wild type Vac14- FLAG (+), or FLAG tagged Vac14 point mutants (+). IPs were done with monoclonal anti-FLAG antibodies and separated by SDS-PAGE and probed as indicated on the left of each blot. For Western blotting, anti-FLAG antibodies were used to confirm immunoprecipitation of Vac14 point mutants and wild type Vac14, while anti-HA antibodies were used to detect whether Vac14-HA was recovered. "*" (asterisk) indicates non-specific bands.

3.6 Effect of Vac14 mutations on Fab1 and Fig4

To test whether monomeric Vac14 mutants supports interaction with Fab1 and/or Fig4, two Vac14 point mutants, *vac14*^{SS} and *vac14*^{CRY}, were tested for coIP with Fab1 and Fig4 expressed in *vac14*Δ cells. First, *vac14*^{SS} and *vac14*^{CRY} were transformed into *vac14*Δ Fab1-Myc, a yeast strain in which *VAC14* is deleted and chromosomal *FAB1* is tagged with Myc for detection with monoclonal anti-Myc antibodies. To confirm the interaction of Vac14 with Fab1 and Fig4, wild type Vac14-FLAG was also transformed into the same yeast strain (*vac14*Δ-Fab1-myc) and used as a control for the interaction. The coIP analysis showed that *Vac14*^{SS} and *Vac14*^{CRY} were unable to interact with Fab1 and Fig4 in comparison to wild type Vac14 (Figure 3.12). This demonstrates that Vac14 multimerization is a prerequisite for Vac14 to bind to Fab1 and Fig4, and consequently Fab1 complex assembly.

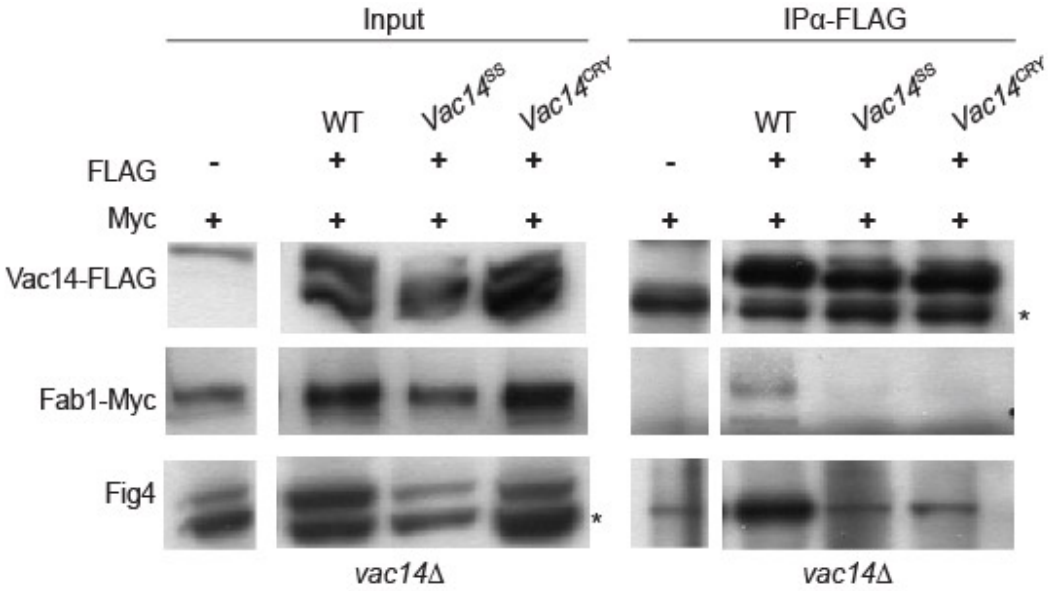

Figure 3.12. Monomeric Vac14 point mutants disrupt interaction with Fab1 and Fig4. IPs were done with monoclonal anti-FLAG antibodies as described in Materials and Methods. IPs were separated by SDS-PAGE and probed as indicated on the left of each blot. Input lanes represent 20% of total protein used for the IP experiment. Whole cell lysates were obtained from *vac14*Δ cells expressing Fab1-myc and transformed with empty vector (-), or with wild type Vac14- FLAG (+), or FLAG-tagged Vac14 point mutants (+). For Western blotting, anti-FLAG antibodies were used to confirm immunoprecipitation of Vac14 point mutants and wild type Vac14, while anti-Myc and anti-Fig4 antibodies were used to detect whether Fab1 and Fig4 was recovered. "*" (asterisk) indicates non-specific

3.7 Effect of Vac14 point mutants on vacuole morphology

In the absence of Vac14, *vac14*Δ cells exhibit large, single lobed vacuoles as a result of the low level of PtdIns(3,5)P_2 (Figure 3.13A). In contrast, wild type cells normally have small multi-lobed vacuoles. To test the functional relevance of Vac14 multimerization, vacuoles in *vac14*Δ cells expressing the Vac14 point mutants were stained with CMAC and observed by fluorescence microscopy to assess rescue of vacuolar morphology. The current study demonstrated that the enlarged vacuoles in *vac14*Δ cells were rescued by the expression of *VAC14* (Figure 3.13B). By comparison, expression of Vac14 point mutants including *vac14*^{SS}, *vac14*^{SIA}, *vac14*^{651CRY} and *vac14*^{NG} were unable to rescue the large single-lobed vacuoles; the four Vac14 point mutants were observed to have similar phenotypes to those seen in *vac14*Δ cells. This suggests that Vac14 multimerization is essential for normal vacuolar morphology and likely PtdIns(3,5)P_2 synthesis (Figure 3.13C-F).

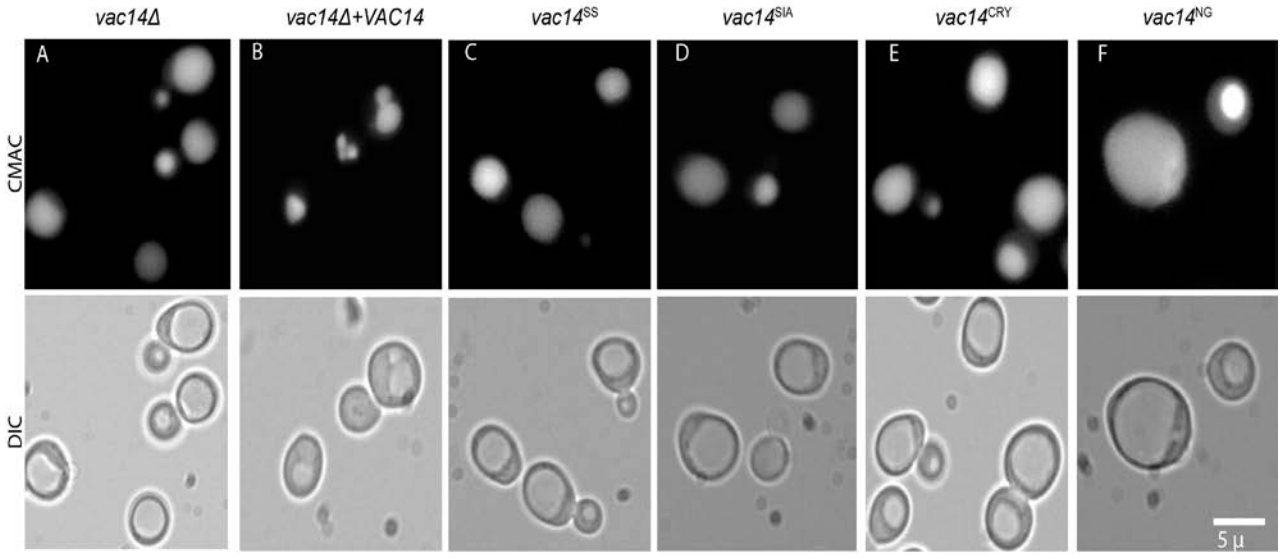

Figure 3.13 Vacuolar morphology of Vac14 point mutants. Images of vacuolar morphology of *vac14*Δ cells (A), *vac14*Δ cells expressing wild type and (B) designated *vac14* point mutants, *vac14*^{SS}, *vac14*^{SIA}, *vac14*^{651CRY} and *vac14*^{NG} (C-F) are shown. Cells were labeled with 100 nM of 4-chloromethyl-7-aminocoumarin (Cell Tracker Blue CMAC) for 10 min which selectively stains the lumen of the yeast vacuoles. DIC: Differential interference contrast microscopy. Scale bare is shown.

4 Discussion

PtdInsPs play a crucial role in the regulation of many cellular functions. The intracellular levels of PtdInsPs are precisely regulated by specific PtdInsP kinases and phosphatases. The recently identified phospholipid (PtdIns(3,5)P_2) is involved in several cellular processes such as endolysosomal trafficking, autophagy and ion channel activity. PtdIns(3,5)P_2 is predominantly synthesized by phosphorylation at the 5-position of PtdIns(3)P by Fab1/PIKfyve (Gary et al, 1998; Rutherford et al, 2006; Ikonomov et al, 2009). Improper regulation of PtdIns(3,5)P_2 levels have been linked to neuropathalogical disorders such as Charcot-Marie-Tooth disease (CMTD) and amyotrophic lateral sclerosis (ALS) (Chow et al., 2009; Chow et al., 2007; Zhang et al., 2008). Despite the significance of PtdIns(3,5)P_2, the exact regulation mechanism that is involved in its synthesis and turnover is yet to be understood. The Fab1 kinase and the Fig4 phosphatase are essential components of the regulatory network that maintain the normal levels of PtdIns(3,5)P_2. Both Fab1 and Fig4 are regulated by Vac14, which acts as an adaptor protein for both enzymes and together they form the Fab1 complex required for proper regulation of PtdIns(3,5)P_2 levels (Jin et al., 2008; Botelho et al., 2008).

Previous studies in yeasts and mammals showed that Vac14 forms a multimer through self-interaction. However, many questions remained unanswered including the multimerization state, the motifs of Vac14 necessary for self-interaction and the functional relevance for multimerization. Using coIP analysis of yeast cell lysates expressing truncations and point mutants of Vac14, this study proposes that Vac14 self-interacts through multiple motifs in the C-terminus. The results of this study also show that disruption of Vac14 multimerization blocks its interaction with Fab1 and Fig4. Consequently, cells expressing monomeric Vac14 mutants

displayed enlarged and single-lobed vacuoles, the abnormal vacuolar morphology caused by PtdIns(3,5)P_2 deficiency.

4.1 Vac14 self-interaction is mediated by conserved motifs in the C-terminus

The previous study using cross-linking of mammalian cells overexpressing ArPIKfyve, the mammalian Vac14 (782 residues), suggested that Vac14 forms a dimer or trimer (Sbrissa et al., 2008). Though the cross-linked bands observed in Western blot were compatible with two or three monomers, this could be due to presence of other endogenous binding proteins associated with Vac14/ArPIKfyve (Sbrissa et al., 2008). However, in the Master's thesis research by Ho, purified recombinant Vac14 was used instead to avoid issues of endogenous binding partners in yeast. Using this system, Ho proposed that Vac14 exists as either a homodimer or trimer (Ryerson, 2011). However, Vac14 appears to have a large Stock's radius; thus, likely Vac14 is a dimer (Ho, Ryerson, 2011). Although Vac14 was known to exist as a multimer, the domain responsible for multimer formation was not known.

In this study, the responsible region for Vac14-self interaction was first estimated using N-terminal and C-terminal Vac14 truncated mutants. Our coIP analysis of the expressed Vac14 truncations with wild-type Vac14 showed that the N-terminal truncated mutant VN4 (residues 350 -880) was sufficient to interact with wild type Vac14 whereas VN5 (residues 436-880) was not as efficient as VN4 (Figure 3.5). In retrospect, the inefficiency of the interaction between VN5 and wild type Vac14 is possibly due to disruption of the HEAT repeat (residues 387-466), which may have caused the remaining N-terminal region to fold improperly over an extended area (Figure 3.12). In contrast, the C-terminal VC5 (residues 1-600) in which the minimal predicted HEAT repeats remained intact (Figure 3.1), failed to interact with wild type Vac14.

This suggests that the C-terminal Vac14 is crucial for the self-interaction (Figure 3. 6). Our findings appear to be consistent with earlier observation with the mammalian Vac14 (Sbrissa et al., 2008). The homomeric interaction of Vac14 in mammalian cells was revealed to be mediated by the C-terminal (residues 523 to 782). However, the precise motifs involved in the homomeric interaction have not been determined (Sbrissa et al., 2008).

Based on these observations, we identified the C-terminus of yeast Vac14 (residues 500-880) as the likely region for Vac14 self-interaction. To further identify the potential motifs in the C-terminus responsible for Vac14 multimerization, point mutations in the C-terminal region above were generated by site-directed mutagenesis in the most conserved motifs identified by the multiple sequence alignment of Vac14 orthologs from diverse organisms (Figure 3.7). The constructed Vac14 point mutants included *vac14*^{560SS}, *vac14*^{623SIA}, *vac14*^{651CRY} and *vac14*^{582NG} and were expressed in yeast cells, followed by coIP to test for interaction with wild type Vac14. Though *vac14*^{623SIA}, *vac14*^{651CRY} showed lower steady-state expression levels compared to wild type Vac14, these variations can be overcome in pull-down independently of expression levels

As shown earlier, the coIP analysis suggested that the amino acid residues including F560, L564, I582, R584 and S651, W652 C653, appear to be the most critical consensus sequences for Vac14 multimerization. The amino acid residues L623, T625 and E628, located within highly conserved motif, seem to be also involved in the multimerization of Vac14. However, mutations of this motif partially disrupt Vac14 self-interaction, suggesting that other motifs play a more important role in stabilizing Vac14-Vac14 interaction. The possible orientation of Vac14 multimerization in the Fab1 complex is discussed later.

The interaction between Vac14 point mutants and wild type Vac14 was also tested *in vitro* using bacterially expressed recombinant Vac14. The interaction of wild type Vac14 with itself was confirmed in vitro and used as a control. However, the in vitro binding assay showed no direct interaction between Vac14 point mutants and wild type Vac14 (Figure 4.1) (Ho, 2011, unpublished). These observations are consistent with the coIP analysis of Vac14 point mutants. Moreover, in a yeast-two hybrid test, the N-terminal Vac14 point mutant (L149R) did not affect Vac14 self-interaction (Jin et al., 2008). Collectively, these observations suggest that the identified conserved motifs on the C-terminus are responsible for Vac14 self-interaction.

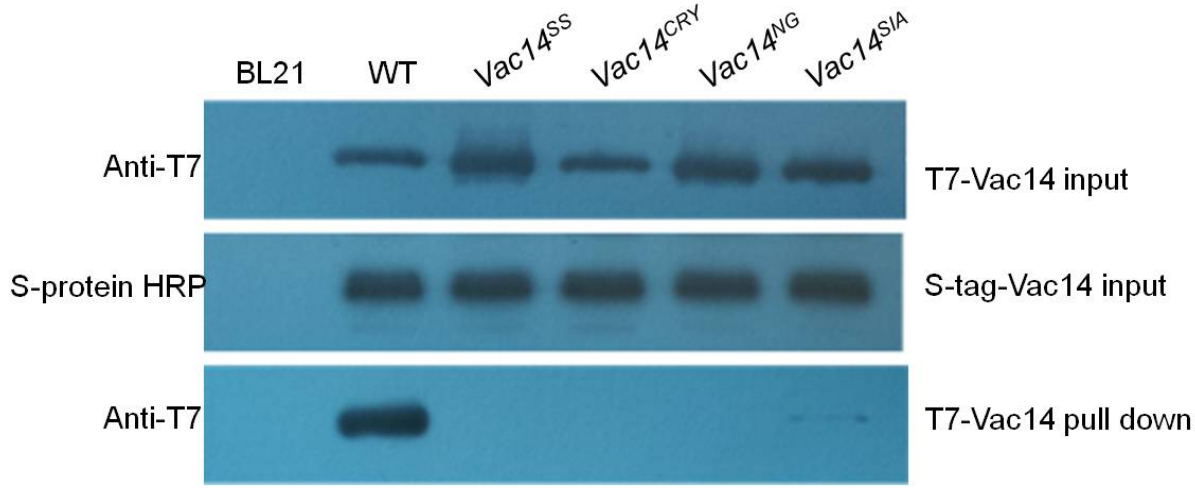

Figure 4.1. In-vitro Vac14 self-interaction. Purified S-tag-Vac14 coated on S-protein agarose beads were incubated with purified recombinant T7-Vac14-HIS and recombinant T7-Vac14-HIS point mutants: $Vac14^{SS}$, $Vac14^{CRY}$, $Vac14^{NG}$, $Vac14^{SIA}$. Input represents 20% of the total purified recombinant wild-type and point mutant T7-Vac14-HIS and S-tag Vac14 used. T7-Vac14 pull down represent total recombinant T7-Vac14-HIS pulled down by S-tag-Vac14 detected by Western blot with α-T7 antibodies (Ho, 2011).

To further characterize the proposed motifs that mediate Vac14 multimerization, we attempted to use REP, a repeat finding program to see whether these motifs are located within proposed HEAT repeats (Jin et al., 2008). However, based on previous analysis of Vac14 amino acid sequence, one of the potential motifs (residues F560 and L564) is located within a HEAT

repeat (516-592) (Jin et al., 2008). In addition, the multiple alignments of Vac14 sequence indicated that this motif is part of a conserved leucine-rich repeat. The leucine-rich repeat is one of the major repeat families that commonly form complexes with other proteins and mediate essential cellular functions such as signal transduction and cell adhesion (Andrade et al., 2001). This supports a major role for the first identified motif (residues F560 and L564) in Vac14-multimerization possibly by binding with other regulatory components. The remaining identified motifs (residues I582, R584, L623, T625, E628 and S651, W652, C653) are also within highly conserved region of the C-terminus of Vac14. The sequence analysis of the mammalian Vac14 (or ArPIKfyve) showed that the conserved C-terminal domain that mediate homomeric interaction of Vac14/ ArPIKfyve was not predicted to contain HEAT repeats (Sbrissa et al., 2008). However, different sequence analysis by Jin et al. predicted that Vac14 contains 21 and 17 HEAT repeats in yeast and mammals, respectively (2008). Importantly, there are precedents that show that HEAT repeats mediate homo-dimerization – for example that of PP2A, a protein phosphatase 2A, whose structure is shown in Figure 4.2A.

Based on the presented data, we propose two models of Vac14 self-interaction: Vac14 self interacts in either a parallel or an anti-parallel manner via the identified motifs in the C-terminus. In the parallel dimerization, the C-terminal ends of Vac14 interact while the N-termini remain unbound. In comparison, in the anti-parallel dimerization model, the C-terminal ends bind in opposing orientation while the N-termini are exposed at the far ends. The N-terminal ends are not likely to contribute to binding since VN4 retrieved the interaction. The possible orientations for Vac14 dimerization are shown in Figure 4.2.B. Future work will be required to address these two possibilities.

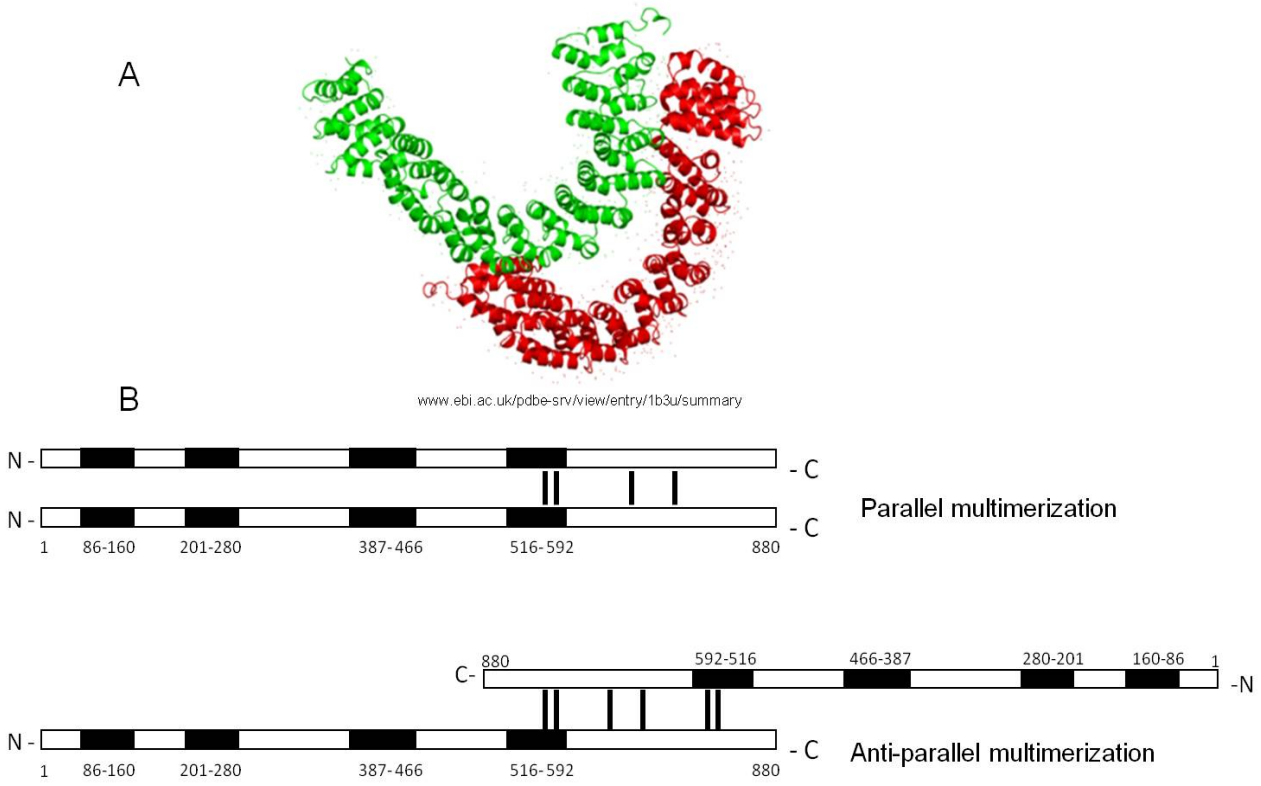

Figure 4.2: Models of Vac14 multimer. A. Anti-parallel dimerization of Protein Phosphatase 2A subunits (PP2A), which contains 15 HEAT repeats. Two subunits, A (red) and B (green) are shown. **B.** Schematic diagram represent two possible orientations of Vac14 dimer. The black boxes represent the high-confidence predicted HEAT repeats. The numbers of the amino acid residues are shown.

4.2 Multimeric Vac14 is required for interaction with Fab1 and Fig4

In yeast and in mammals, Vac14 binds to both the Fab1 kinase and the Fig4 phosphatase to form the Fab1 complex that is essential for regulation of PtdIns(3,5)P_2 levels (Jin et al., 2008; Botelho et al. ; Sbrissa et al., 2007) . In addition, yeast two-hybrid analysis and/or co-IP showed that Vac14 also interacts with Vac7 and Atg18, which are positive and negative regulators of Fab1, respectively (Jin et al., 2008). Therefore, Vac14 forms the core of the Fab1 complex by forming a dimer and integrating Fab1, Fig4, Vac7 and possibly Atg18. Indeed, whereas *vac14*Δ cells did not maintain Fab1 and Fig4 interaction, *vac7*Δ and *atg18*Δ cells retained the Fab1-Fig4

interaction, showing that Fab1 and Fig4 bind independently of Vac7 or Atg18 (Botelho et al., 2008). Additionally, the mammalian orthologs of Vac14, Fab1 and Fig4 were suggested to be sufficient to form stable ternary complex in mammals (Sibrissa et al., 2007; Sbrissa et al., 2008).

The exact structure and positioning of these regulatory proteins remains to be understood, However, as stated above Vac14 acts as scaffolding protein that provides docking sites for both antagonizing enzymes (Jin et al., 2008; Botelho et al., 2008). A point mutation in HEAT repeat 4 of Vac14 (L149R) in the N-terminus disrupts Vac14-Fab1 interaction, suggesting that the N-terminal region of Vac14 contains a binding site for Fab1, in which Vac14 activates Fab1 to promote PtdIns(3,5)P_2 synthesis (Jin et al., 2008). Interestingly, the C-terminus of Vac14 was already implicated in binding Fig4 and suggested to be important for the stability of the Fab1 complex (Botelho et al., 2008; Ikonomov et al., 2010; Jin et al., 2008, Sbrissa et al, 2007). Here, we precisely identify C-terminal motifs required for Vac14-Vac14 interaction. However, we show that the monomeric Vac14 point mutants *vac14*^{560SS} and *vac14*^{651CRY} were also unable to interact with Fab1 and Fig4. It is unlikely that this is due to direct role of these motifs in Fab1 and/or Fig4 interaction. Rather, we propose that Vac14 self-interaction is a prerequisite for interaction with Fig4 and Fab1. In turn, this implies that the Vac14 dimer is necessary for the assembly of the Fab1 complex, which would be consistent with its proposed role as the core of the Fab1 complex (Jin et al., 2008).

We have conceived two models of how Vac14 dimer might form the Fab1 complex, depending on the orientation of Vac14 multimer. In the first model, Vac14 dimerizes in parallel through the C-termini (Figure 4.2A). The dimer is then required to form a single interface for each Fab1 and Fig4 binding. This is because Fab1 and Fig4 exist as monomers in the Fab1

complex and the Vac14 self-interaction is required to support these interactions (Botelho et al., 2008). Moreover, we position Fab1 and Fig4 in the N-terminal and C-terminal regions of Vac14 based on Jin et al. (2008). We also propose that Fig4 binding to the Vac14 dimer induces a conformational change on the N-terminal region of the Vac14 dimer to bind Fab1 – this is because Fig4 is necessary for Fab1-Vac14 interaction (Botelho et al, 2008) (Figure 4.3A). In the second model, Vac14 self-interacts in an anti-parallel manner. Fig4 still binds to the C-termini region of the Vac14 dimer. We postulate that then this causes a conformational change in the Vac14 dimer that forms an optimal interface to bind Fab1 (Figure 4.3B).

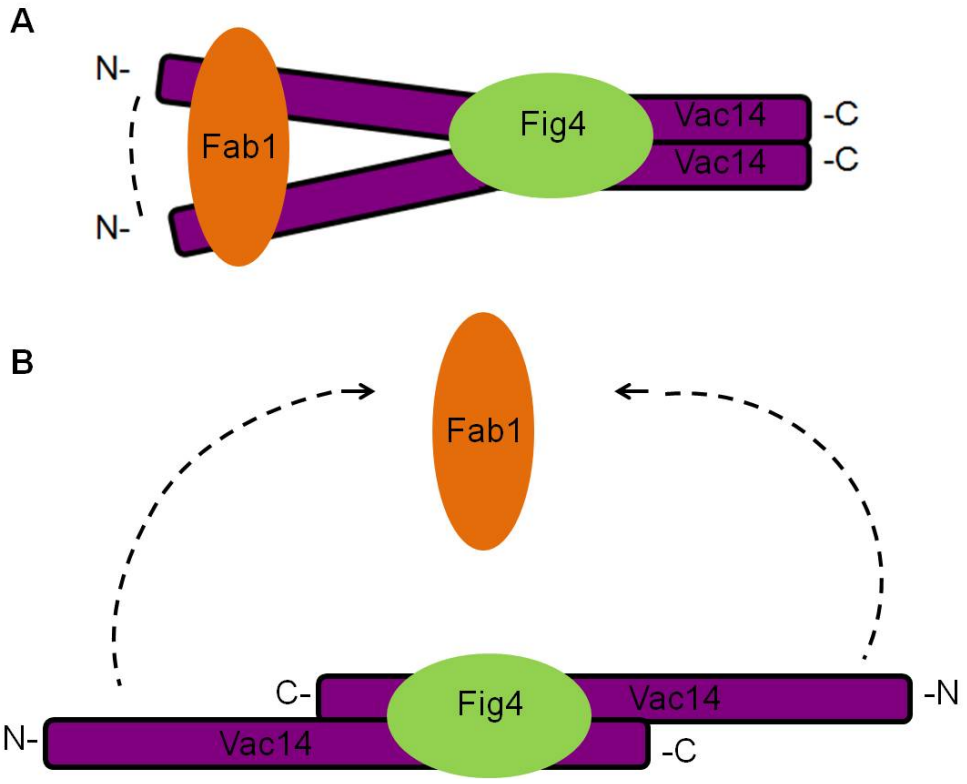

Figure 4.3. Models of Vac14 multimer in the Fab1 complex. Two schematic diagrams show the possible orientation of Vac14 dimer, Fig4 and Fab1 in the Fab1 complex **A.** Parallel dimerization of Vac14 via its C-termini. Vac14 dimer provides binding sites for Fig4, which stabilize the binding of Fab1 to the N-termini of Vac14. **B.** Anti-parallel dimerization occurs via the C-termini of Vac14 leaving the N-termini on opposite ends. Fig4 binds to the C-termini of Vac14, which promotes a conformational change that allows structural rearrangement of the N-termini of Vac14 to interact with Fab1. Dotted lines represent direction of the conformational change initiated by Fig4.

4.3 Disruption of Vac14 multimer affects vacuolar morphology

Vac14 is necessary to maintain the PtdIns(3,5)P_2 levels required for the normal function and morphology of yeast vacuoles. Deletion of *VAC14* decreases the levels of PtdIns(3,5)P_2 by 90 % and cells exhibit single-lobed and enlarged vacuoles compared to wild type (Figure 3.12) (Bonangelino et al., 2002; Dove et al., 2002). To further test the functional relevance of Vac14 multimer at the cellular level, the monomeric Vac14 point mutants were tested for rescue of the *vac14*Δ cells phenotype. As indicated in Figure 3.12, the monomeric Vac14 point mutants failed to rescue the abnormal morphology of the vacuoles. This observation is consistent with the coIP analysis, which suggests that Vac14 dimerization plays a critical role in the assembly of the Fab1 complex. The incapability of the monomeric Vac14 point mutants to rescue the large vacuoles in *vac14*Δ cells is almost certainly due to their failure to interact with Fab1 and Fig4 and maintain the PtdIns(3,5)P_2.

5 Conclusions and Future work

Previous studies shed light on the importance of Vac14 for PtdIns(3,5)P_2 regulation. This study provides molecular insight into the importance of Vac14 self-interaction. First, I identified several motifs that likely mediate Vac14 self-interaction. Second, I showed that monomeric Vac14 mutants do not support interaction with Fab1 and Fig4 interaction. And third, I showed that monomeric Vac14 mutants cannot rescue *vac14*Δ vacuolar defects. Therefore, the Vac14 self-interaction, which likely forms a Vac14 dimer, is a core event that links together the essential regulatory proteins Fab1 and Fig4, which is required for the proper regulation of PtdIns(3,5)P_2 levels. Nevertheless, there remain numerous questions about the role of Vac14 self-interaction and how this interfaces with Fab1 and Fig4 and other regulatory subunits such as Vac7. Importantly, it will be worth investigating the three-dimensional structure of Vac14. The following are proposed approaches to further elucidate on the role of Vac14 multimer.

5.1 Effect of Vac14 multimer on PtdIns(3,5)P_2 levels

As shown before, disruption of the Vac14 multimer prevented rescue of the abnormal vacuolar morphology in *vac14*Δ cells, most likely due to disassembly of the Fab1 complex. To confirm the functional relevance of the Vac14 multimer, cellular levels of PtdIns(3,5)P_2 can be measured in *vac14*Δ cells expressing Vac14 point mutants by labeling in vivo PtdInsPs with [^{3}H]-inositol. The radiolabeled lipids are then extracted, deacylated and followed by separation by High-performance liquid chromatography (HPLC). In HPLC, the deacylated extracts are passed through an ion-exchange column, which fractionates each PtdInsP species based on differential interaction with the column. The eluant is then passed through a flow scintillator that quantifies radioactive signal, which in turn indicates how much PtdInsP there was in the cell

(Zhang and Buxton, 1998, Botelho et al., 2008). Comparing the levels of PtdIns(3,5)P_2 in *vac14*Δ cells expressing monomeric Vac14 versus multimeric Vac14 should provide better understanding of how Vac14 multimerization involved in PtdIns(3,5)P_2 regulation. This is important because not all situations that lead to large vacuoles is due to low PtdIns(3,5)P_2. For example, in *atg18*Δ cells, the vacuoles are enlarged and singled-lobed but PtdIns(3,5)P_2 is 10-fold higher than in wild-type cells (Dove et al., 2004; Efe et al., 2007).

5.2 Identification of Vac14 structure

Despite the important role of Vac14 in regulating the levels of PtdIns(3,5)P_2, its structure has not been identified. Ideally, the structure of Vac14 could be determined by X-ray crystallography, which is widely used to provide high-resolution atomic structure of molecules including proteins. In this method, recombinant Vac14 would be purified in high-quality yield and crystallized. Crystals are then bombarded with X-rays to create a diffraction pattern that can be interpreted into a protein structure (Smyth and Martin, 2000). Analysis of the amino acid sequences of Vac14 together with its structure could produce a precise model of Vac14 multimer structure. Elucidation of the detailed structure of Vac14 would help provide a clear understanding of Vac14 functions. Nevertheless, protein structure determination is not trivial and would require considerable amount of optimization.

References

Anderson, N. G. (1998). Co-immunoprecipitation. *Methods Mol.Biol, 88*, 35-45.

Andrade, M. A., Petosa, C., O'Donoghue, S. I., Müller, C. W., & Bork, P. (2001). Comparison of ARM and HEAT protein repeats1. *Journal of Molecular Biology, 309*(1), 1-18.

Behnia, R., & Munro, S. (2005). Organelle identity and the signposts for membrane traffic. *Nature, 438*(7068), 597-604.

Bonangelino, C. J., Nau, J. J., Duex, J. E., Brinkman, M., Wurmser, A. E., Gary, J. D., Weisman, L. S. (2002). Osmotic stress–induced increase of phosphatidylinositol 3, 5-bisphosphate requires Vac14p, an activator of the lipid kinase Fab1p. *The Journal of Cell Biology, 156*(6), 1015-1028.

Bonifacino, J. S., & Glick, B. S. (2004). The mechanisms of vesicle budding and fusion. *Cell, 116*(2), 153-166.

Botelho, R. J., Efe, J. A., Teis, D., & Emr, S. D. (2008). Assembly of a Fab1 phosphoinositide kinase signaling complex requires the Fig4 phosphoinositide phosphatase. *Molecular Biology of the Cell, 19*(10), 4273-4286.

Bryant, N. J., & Stevens, T. H. (1998). Vacuole biogenesis in saccharomyces cerevisiae: Protein transport pathways to the yeast vacuole. *Microbiology and Molecular Biology Reviews, 62*(1), 230.

Burd, C. G., & Emr, S. D. (1998). Phosphatidylinositol (3)-phosphate signaling mediated by specific binding to RING FYVE domains. *Molecular Cell, 2*(1), 157-162.

Cheng, X., Shen, D., Samie, M., & Xu, H. (2010). Mucolipins: Intracellular TRPML1-3 channels. *FEBS Letters, 584*(10), 2013-2021.

Chow, C. Y., Landers, J. E., Bergren, S. K., Sapp, P. C., Grant, A. E., Jones, J. M., Weisman, L. S. (2009). Deleterious variants of FIG4, a phosphoinositide phosphatase, in patients with ALS. *The American Journal of Human Genetics, 84*(1), 85-88.

Chow, C. Y., Zhang, Y., Dowling, J. J., Jin, N., Adamska, M., Shiga, K., Zhang, X. (2007). Mutation of FIG4 causes neurodegeneration in the pale tremor mouse and patients with CMT4J. *Nature, 448*(7149), 68-72.

Cooke, F. T., Dove, S. K., McEwen, R. K., Painter, G., Holmes, A. B., Hall, M. N., Parker, P. J. (1998). The stress-activated phosphatidylinositol 3-phosphate 5-kinase Fab1p is essential for vacuole function in S. cerevisiae. *Current Biology, 8*(22), 1219-1222, S1-S2.

Di Paolo, G., & De Camilli, P. (2006). Phosphoinositides in cell regulation and membrane dynamics. *Nature, 443*(7112), 651-657.

Doherty, G. J., & McMahon, H. T. (2009). Mechanisms of endocytosis. *Annual Review of Biochemistry, 78*, 857-902.

Dong, X., Shen, D., Wang, X., Dawson, T., Li, X., Zhang, Q., . . . Delling, M. (2010). PI (3, 5) P2 controls membrane trafficking by direct activation of mucolipin Ca2 release channels in the endolysosome. *Nature Communications, 1*, 38.

Dove, S. K., Cooke, F. T., Douglas, M. R., Sayers, L. G., Parker, P. J., & Michell, R. H. (1997). Osmotic stress activates phosphatidylinositol-3, 5-bisphosphate synthesis. *Nature, 390*(6656), 187-192.

Dove, S. K., McEwen, R. K., Mayes, A., Hughes, D. C., Beggs, J. D., & Michell, R. H. (2002). Vac14 controls PtdIns (3, 5) P2 synthesis and Fab1-dependent protein trafficking to the multivesicular body. *Current Biology, 12*(11), 885-893.

Dove, S. K., Piper, R. C., McEwen, R. K., Yu, J. W., King, M. C., Hughes, D. C., Michell, R. H. (2004). Svp1p defines a family of phosphatidylinositol 3, 5-bisphosphate effectors. *The EMBO Journal, 23*(9), 1922-1933.

Duex, J. E., Nau, J. J., Kauffman, E. J., & Weisman, L. S. (2006). Phosphoinositide 5-phosphatase Fig4p is required for both acute rise and subsequent fall in stress-induced phosphatidylinositol 3, 5-bisphosphate levels. *Eukaryotic Cell, 5*(4), 723-731.

Duex, J. E., Tang, F., & Weisman, L. S. (2006). The Vac14p–Fig4p complex acts independently of Vac7p and couples PI3, 5P2 synthesis and turnover. *The Journal of Cell Biology, 172*(5), 693-704.

Efe, J. A., Botelho, R. J., & Emr, S. D. (2005). The Fab1 phosphatidylinositol kinase pathway in the regulation of vacuole morphology. *Current Opinion in Cell Biology, 17*(4), 402-408.

Efe, J. A., Botelho, R. J., & Emr, S. D. (2007). Atg18 regulates organelle morphology and Fab1 kinase activity independent of its membrane recruitment by phosphatidylinositol 3, 5-bisphosphate. *Molecular Biology of the Cell, 18*(11), 4232-4244.

Gary, J. D., Sato, T. K., Stefan, C. J., Bonangelino, C. J., Weisman, L. S., & Emr, S. D. (2002). Regulation of Fab1 phosphatidylinositol 3-phosphate 5-kinase pathway by Vac7 protein and Fig4, a polyphosphoinositide phosphatase family member. *Molecular Biology of the Cell, 13*(4), 1238-1251.

Gary, J. D., Wurmser, A. E., Bonangelino, C. J., Weisman, L. S., & Emr, S. D. (1998). Fab1p is essential for PtdIns (3) P 5-kinase activity and the maintenance of vacuolar size and membrane homeostasis. *The Journal of Cell Biology, 143*(1), 65-79.

Gonzalez Jr, L., & Scheller, R. H. (1999). Regulation of membrane trafficking: Structural insights from a Rab/effector complex. *Cell, 96*(6), 755.

Guo, S., Stolz, L. E., Lemrow, S. M., & York, J. D. (1999). SAC1-like domains of yeast SAC1, INP52, and INP53 and of human synaptojanin encode polyphosphoinositide phosphatases. *Journal of Biological Chemistry, 274*(19), 12990.

Ho, Shannon Cheuk Ying (2011). In Ryerson University. School of Graduate Studies. Program of Molecular Science. (Ed.), *Characterizing the VAC14 multimeric state*

Honing, S., Ricotta, D., Krauss, M., Spate, K., Spolaore, B., Motley, A., Owen, D. J. (2005). Phosphatidylinositol-(4, 5)-bisphosphate regulates sorting signal recognition by the clathrin-associated adaptor complex AP2. *Molecular Cell, 18*(5), 519-531.

Hurley, J. H., & Misra, S. (2000). Signaling and subcellular targeting by membrane-binding domains 1. *Annual Review of Biophysics and Biomolecular Structure, 29*(1), 49-79.

Ikonomov, O. C., Sbrissa, D., Fenner, H., & Shisheva, A. (2009). PIKfyve-ArPIKfyve-Sac3 core complex. *Journal of Biological Chemistry, 284*(51), 35794.

Ikonomov, O. C., Sbrissa, D., Fligger, J., Delvecchio, K., & Shisheva, A. (2010). ArPIKfyve regulates Sac3 protein abundance and turnover. *Journal of Biological Chemistry, 285*(35), 26760-26764.

Ikonomov, O. C., Sbrissa, D., Foti, M., Carpentier, J. L., & Shisheva, A. (2003). PIKfyve controls fluid phase endocytosis but not recycling/degradation of endocytosed receptors or sorting of procathepsin D by regulating multivesicular body morphogenesis. *Molecular Biology of the Cell, 14*(11), 4581-4591.

Ikonomov, O. C., Sbrissa, D., Mlak, K., Kanzaki, M., Pessin, J., & Shisheva, A. (2002). Functional dissection of lipid and protein kinase signals of PIKfyve reveals the role of PtdIns 3, 5-P2 production for endomembrane integrity. *Journal of Biological Chemistry, 277*(11), 9206-9211.

Ikonomov, O. C., Sbrissa, D., & Shisheva, A. (2001). Mammalian cell morphology and endocytic membrane homeostasis require enzymatically active phosphoinositide 5-kinase PIKfyve. *Journal of Biological Chemistry, 276*(28), 26141.

Jin, N., Chow, C. Y., Liu, L., Zolov, S. N., Bronson, R., Davisson, M., . . . Duex, J. E. (2008). VAC14 nucleates a protein complex essential for the acute interconversion of PI3P and PI (3, 5) P2 in yeast and mouse. *The EMBO Journal, 27*(24), 3221-3234.

Katzmann, D. J., Odorizzi, G., & Emr, S. D. (2002). Receptor downregulation and multivesicular-body sorting. *Nature Reviews Molecular Cell Biology, 3*(12), 893-905.

Lange, I., Yamamoto, S., Partida-Sanchez, S., Mori, Y., Fleig, A., & Penner, R. (2009). TRPM2 functions as a lysosomal Ca2 -release channel in β cells. *Science Signaling, 2*(71), ra23.

Martin, T. F. J. (2001). PI (4, 5) P2 regulation of surface membrane traffic. *Current Opinion in Cell Biology, 13*(4), 493-499.

Martin, T. (1998). Phosphoinositide lipids as signaling molecules: Common themes for signal transduction, cytoskeletal regulation, and membrane trafficking. *Annual Review of Cell and Developmental Biology, 14*(1), 231-264.

Maxfield, F. R., & McGraw, T. E. (2004). Endocytic recycling. *Nature Reviews Molecular Cell Biology, 5*(2), 121-132.

Mellman, I. (1992). The importance of being acid: The role of acidification in intracellular membrane traffic. *Journal of Experimental Biology, 172*(1), 39-45.

Michell, R. H., Heath, V. L., Lemmon, M. A., & Dove, S. K. (2006). Phosphatidylinositol 3, 5-bisphosphate: Metabolism and cellular functions. *Trends in Biochemical Sciences, 31*(1), 52-63.

Nicot, A. S., Fares, H., Payrastre, B., Chisholm, A. D., Labouesse, M., & Laporte, J. (2006). The phosphoinositide kinase PIKfyve/Fab1p regulates terminal lysosome maturation in caenorhabditis elegans. *Molecular Biology of the Cell, 17*(7), 3062-3074.

Odorizzi, G., Babst, M., & Emr, S. D. (1998). Fab1p PtdIns (3) P 5-kinase function essential for protein sorting in the multivesicular body. *Cell, 95*(6), 847-858.

Piper, R. C., & Luzio, J. P. (2001). Late endosomes: Sorting and partitioning in multivesicular bodies. *Traffic, 2*(9), 612-621.

Polson, H., de Lartigue, J., Rigden, D. J., Reedijk, M., Urbé, S., Clague, M. J., & Tooze, S. A. (2010). Mammalian Atg18 (WIPI2) localizes to omegasome-anchored phagophores and positively regulates LC3 lipidation. *Autophagy, 6*(4)

Proikas-Cezanne, T., Waddell, S., Gaugel, A., Frickey, T., Lupas, A., & Nordheim, A. (2004). WIPI-1α (WIPI49), a member of the novel 7-bladed WIPI protein family, is aberrantly expressed in human cancer and is linked to starvation-induced autophagy. *Oncogene, 23*(58), 9314-9325.

Puertollano, R., & Kiselyov, K. (2009). TRPMLs: In sickness and in health. *American Journal of Physiology-Renal Physiology, 296*(6), F1245-F1254.

Rogers, S. L., & Gelfand, V. I. (2000). Membrane trafficking, organelle transport, and the cytoskeleton. *Current Opinion in Cell Biology, 12*(1), 57-62.

Rudge, S. A., Anderson, D. M., & Emr, S. D. (2004). Vacuole size control: Regulation of PtdIns (3, 5) P2 levels by the vacuole-associated Vac14-Fig4 complex, a PtdIns (3, 5) P2-specific phosphatase. *Molecular Biology of the Cell, 15*(1), 24-36.

Rusten, T. E., & Stenmark, H. (2006). Analyzing phosphoinositides and their interacting proteins. *Nature Methods, 3*(4), 251-258.

Rutherford, A. C., Traer, C., Wassmer, T., Pattni, K., Bujny, M. V., Carlton, J. G., Cullen, P. J. (2006). The mammalian phosphatidylinositol 3-phosphate 5-kinase (PIKfyve) regulates endosome-to-TGN retrograde transport. *Journal of Cell Science, 119*(19), 3944.

Saric, Amra (2009). In Ryerson University. *Toward the Identification of the Vac14 Adaptor protein self-interaction Domain*. (Unpublished Bachelors thesis).

Sbrissa, D., Ikonomov, O. C., Fenner, H., & Shisheva, A. (2008). ArPIKfyve homomeric and heteromeric interactions scaffold PIKfyve and Sac3 in a complex to promote PIKfyve activity and functionality. *Journal of Molecular Biology, 384*(4), 766-779.

Sbrissa, D., Ikonomov, O. C., Fu, Z., Ijuin, T., Gruenberg, J., Takenawa, T., & Shisheva, A. (2007). Core protein machinery for mammalian phosphatidylinositol 3, 5-bisphosphate synthesis and turnover that regulates the progression of endosomal transport. *Journal of Biological Chemistry, 282*(33), 23878.

Sbrissa, D., Ikonomov, O. C., & Shisheva, A. (2000). PIKfyve lipid kinase is a protein kinase: Downregulation of 5'-phosphoinositide product formation by autophosphorylation. *Biochemistry, 39*(51), 15980-15989.

Sbrissa, D., Ikonomov, O. C., & Shisheva, A. (2002). Phosphatidylinositol 3-phosphate-interacting domains in PIKfyve. *Journal of Biological Chemistry, 277*(8), 6073.

Schekman, R., & Orci, L. (1996). Coat proteins and vesicle budding. *Science, 271*(5255), 1526.

Shen, J., Yu, W. M., Brotto, M., Scherman, J. A., Guo, C., Stoddard, C., Qu, C. K. (2009). Deficiency of MIP/MTMR14 phosphatase induces a muscle disorder by disrupting Ca2 homeostasis. *Nature Cell Biology, 11*(6), 769-776.

Simonsen, A., Lippe, R., Christoforidis, S., Gaullier, J. M., Brech, A., Callaghan, J., . . . Stenmark, H. (1998). EEA1 links PI (3) K function to Rab5 regulation of endosome fusion. *Nature, 394*(6692), 494-498.

Touchberry, C. D., Bales, I. K., Stone, J. K., Rohrberg, T. J., Parelkar, N. K., Nguyen, T., . . . Andresen, J. J. (2010). Phosphatidylinositol 3, 5-bisphosphate (PI (3, 5) P2) potentiates cardiac contractility via activation of the ryanodine receptor. *Journal of Biological Chemistry, 285*(51), 40312.

Vetter, I. R., Arndt, A., Kutay, U., & Wittinghofer, A. (1999). Structural view of the ran-importin [beta] interaction at 2.3 resolution. *Cell, 97*(5), 635-646.

Vicinanza, M., D'Angelo, G., Di Campli, A., & De Matteis, M. A. (2008). Function and dysfunction of the PI system in membrane trafficking. *The EMBO Journal, 27*(19), 2457-2470.

Whiteford, C. C., Brearley, C. A., & Ulug, E. (1997). Phosphatidylinositol 3, 5-bisphosphate defines a novel PI 3-kinase pathway in resting mouse fibroblasts. *Biochemical Journal, 323*(Pt 3), 597.

Whyte, J. R. C., & Munro, S. (2002). Vesicle tethering complexes in membrane traffic. *Journal of Cell Science, 115*(13), 2627.

Wishart, M. J., & Dixon, J. E. (2002). PTEN and myotubularin phosphatases: From 3-phosphoinositide dephosphorylation to disease. *Trends in Cell Biology*, *12*(12), 579-585.

Yamamoto, A., Boronenkov, D. B. D. W. I. V., Anderson, R., Emr, S., & Koshland, D. (1995). Novel PI (4) P 5-kinase homologue, Fab1p, essential for normal vacuole function and morphology in yeast. *Molecular Biology of the Cell*, *6*(5), 525.

Zhang, L., & Buxton, I. L. O. (1998). Measurement of phosphoinositols and phosphoinositides using radio high-performance liquid chromatography flow detection. *METHODS IN MOLECULAR BIOLOGY-CLIFTON THEN TOTOWA-*, *105*, 47-64.

Zhang, X., Chow, C. Y., Sahenk, Z., Shy, M. E., Meisler, M. H., & Li, J. (2008). Mutation of FIG4 causes a rapidly progressive, asymmetric neuronal degeneration. *Brain*, *131*(8), 1990-2001.

Zhang, Y., Zolov, S. N., Chow, C. Y., Slutsky, S. G., Richardson, S. C., Piper, R. C., . . . Morrison, S. J. (2007). Loss of Vac14, a regulator of the signaling lipid phosphatidylinositol 3, 5-bisphosphate, results in neurodegeneration in mice. *Proceedings of the National Academy of Sciences*, *104*(44), 17518.

Zhong, R., & Ye, Z. H. (2003). The SAC domain-containing protein gene family in arabidopsis. *Plant Physiology*, *132*(2), 544-555.